

**Waste Mixing and Diluent Selection
for the Planned Retrieval of
Hanford Tank 241-SY-102:
A Preliminary Assessment**

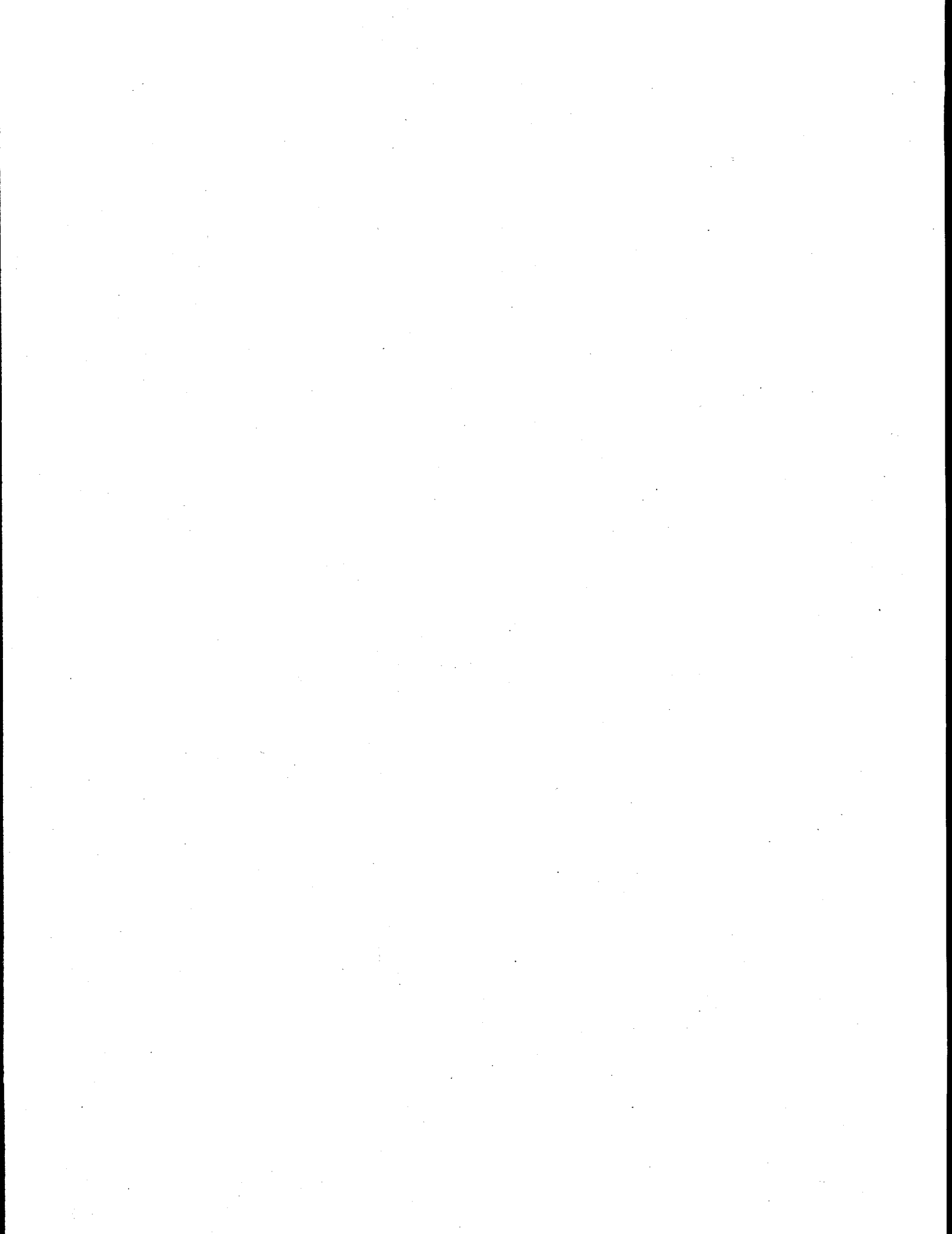
Y. Onishi
J. D. Hudson

January 1996

Prepared for
the U.S. Department of Energy
under Contract DE-AC06-76RLO 1830

Pacific Northwest National Laboratory
Richland, Washington 99352

MASTER



DISCLAIMER

**Portions of this document may be illegible
in electronic image products. Images are
produced from the best available original
document.**

Summary

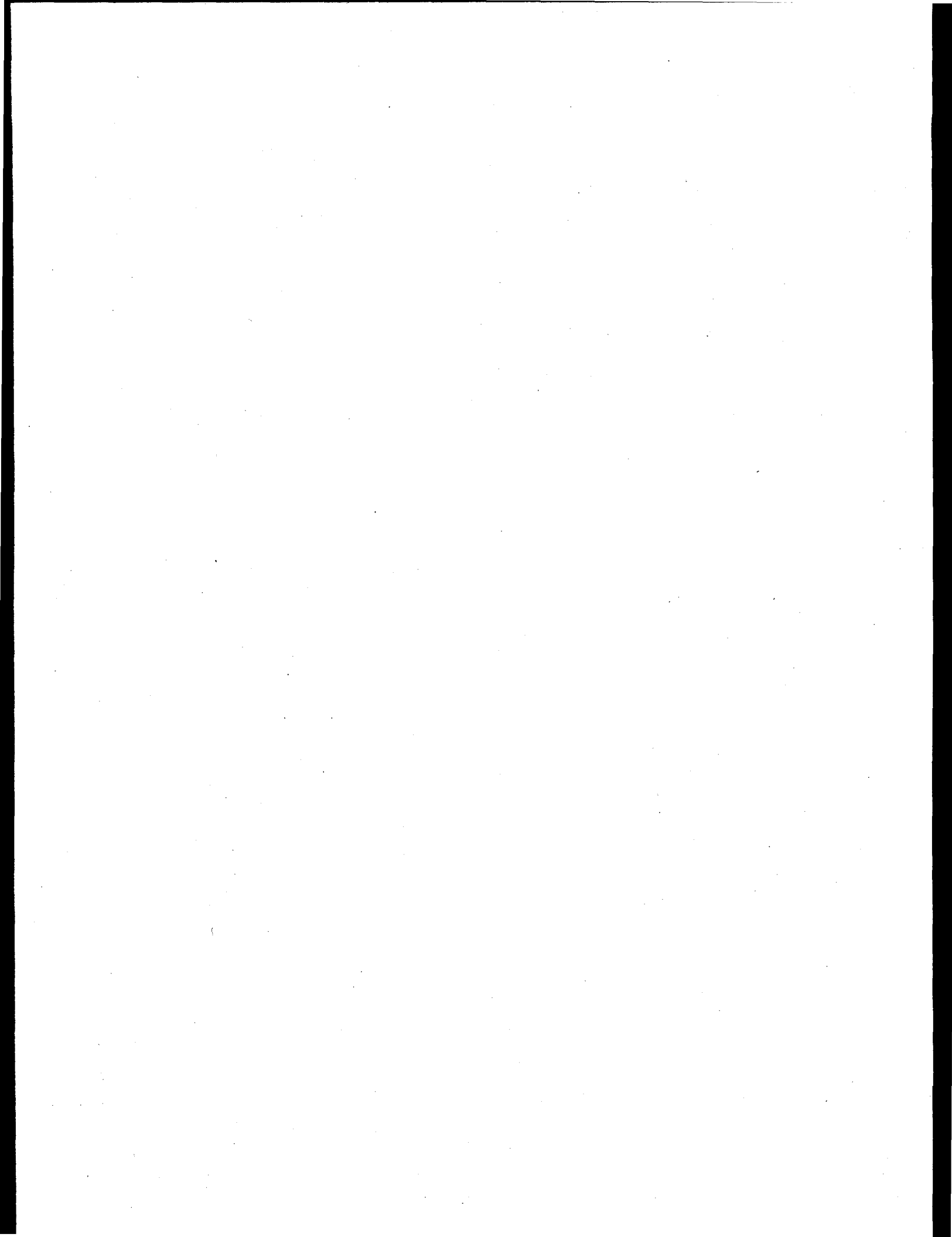
This preliminary assessment documents a set of analyses that were performed to determine the potential for Hanford waste Tank 241-SY-102 waste properties to be adversely affected by mixing the current tank contents or by injecting additional diluent into the tank during sludge mobilization. As a part of this effort, the effects of waste heating that will occur as a result of mixer pump operations are also examined. Finally, the predicted transport behavior of the resulting slurries is compared with the waste acceptance criteria for the Cross-Site Transfer System (CSTS). This work is being performed by Pacific Northwest National Laboratory in support of Westinghouse Hanford Company's W-211 Retrieval Project.

We applied the equilibrium chemical code, GMIN, to predict potential chemical reactions. We examined the potential effects of mixing the current tank contents (sludge and supernatant liquid) at a range of temperatures and, separately, of adding pure water at a volume ratio of 1:2:2 (sludge:supernatant liquid:water) as an example of further diluting the current tank contents. The main conclusion of the chemical modeling is that mixing the sludge and the supernate (with or without additional water) in Tank 241-SY-102 dissolves all sodium-containing solids (i.e., $\text{NaNO}_3(\text{s})$, thenardite, $\text{NaF}(\text{s})$, and halite), but does not significantly affect the amorphous $\text{Cr}(\text{OH})_3$ and calcite phase distribution. A very small amount of gibbsite [$\text{Al}(\text{OH})_3(\text{s})$] might precipitate at 25°C , but a somewhat larger amount of gibbsite is predicted to dissolve at the higher temperatures. Thus gibbsite precipitation might be avoided at moderate temperatures.

In concurrence with the reported tank data, the model affirmed that the interstitial solution within the sludge is saturated with respect to many of the solids species in the sludge, but that the supernatant liquid is not in saturation with many of major solids species in sludge. This indicates that a further evaluation of the sludge mixing could prove beneficial. This type of analysis could provide more detail about the potential chemical reactions and associated rheology changes by incorporating spatial distributions and temporal changes of reactions and kinetics using a model that couples the physical distributions and movements with equilibrium/kinetic chemical reactions and associated rheology changes.

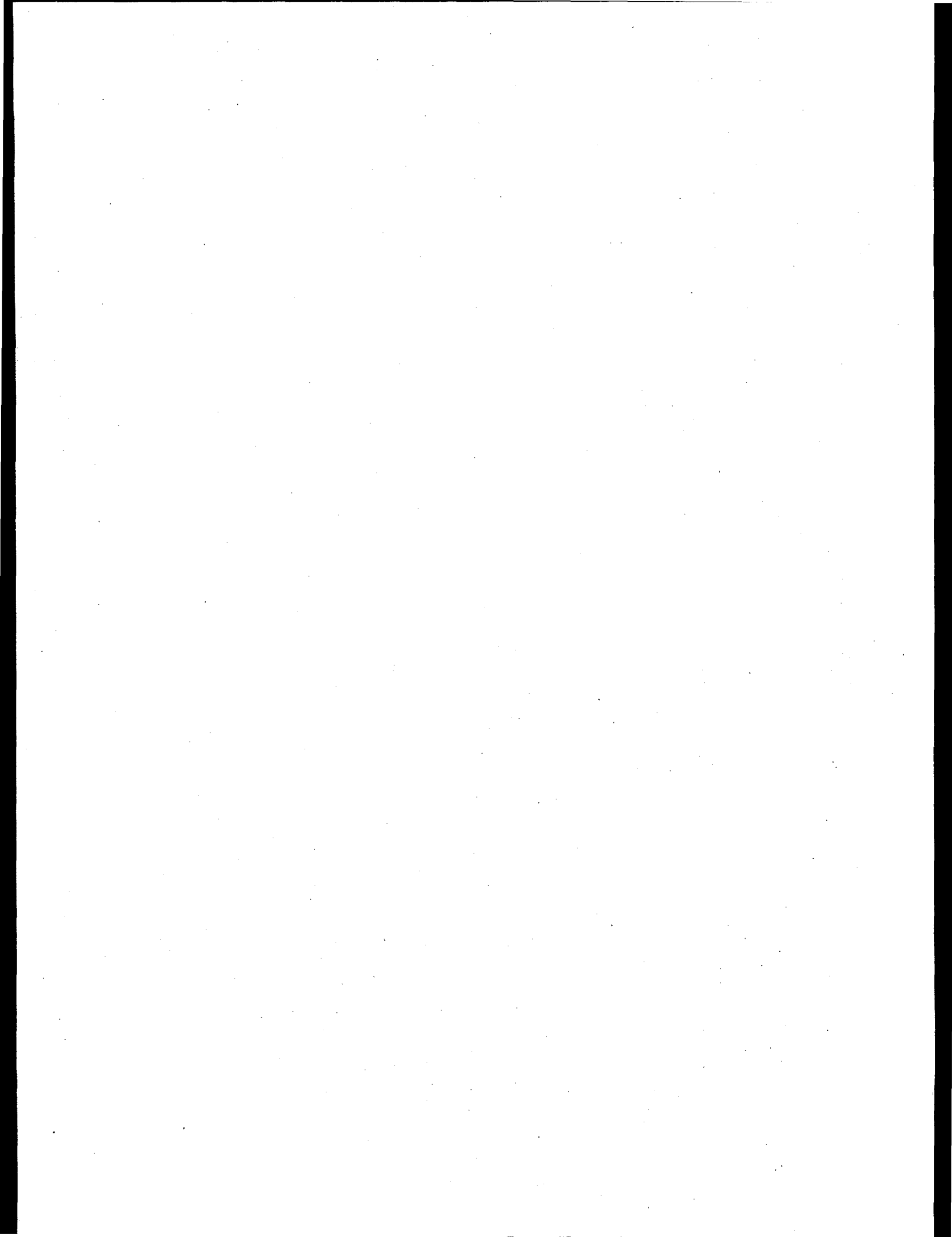
The chemical constituents and phase distributions predicted by the chemical modeling work were also used to predict the transport behavior of the slurries that will result from sludge mobilization in Tank 241-SY-102. Several properties that impact the anticipated waste acceptance criteria for the CSTS were estimated for each of the cases considered. From these estimates it seems clear that the waste slurry that results from sludge mobilization in 241-SY-102 will have a specific gravity less than 1.2, a mixture viscosity less than 30 cP, and a solids volume fraction less than 0.06. Sedimentation data indicate that the "displaced solids volume fraction" is expected to be high for all cases considered.

Estimates of the pressure drop required to maintain particulate suspension during waste transport were also made for each case considered. These indicate that, while higher temperatures result in less solids to transport (due to more solids dissolution), higher pressure drops are required for these cases due to significant (temperature-related) decreases in the liquid viscosity. The maximum pressure drop predicted is less than 500 psi (3500 kPa), while the anticipated system design for the CSTS is approximately 1200 psi.



Acknowledgments

The authors would like to acknowledge many helpful discussions with and suggestions from S. M. Sterner, J. R. Rustad, and A. R. Felmy of Pacific Northwest National Laboratory regarding the chemical modeling and implementation of the GMIN computer code.



Contents

Summary	iii
Acknowledgments	1.1
1.0 Introduction	1.1
2.0 Tank Waste Chemistry	2.1
2.1 Background	2.1
2.1.1 Aluminum Phases	2.1
2.1.2 Phosphates	2.2
2.1.3 Iron, Lead, and Manganese	2.4
2.2 Chemical Modeling Approach	2.4
2.3 Chemistry Of Sludge	2.5
2.3.1 Aqueous and Solid Species Measurements	2.5
2.3.2 Aqueous Species Selection	2.5
2.3.3 Selection of Appropriate Solids	2.6
2.3.4 Combined Solid Cases	2.10
2.4 Mixture of Sludge and Supernate at Temperature 25°C for Case 1	2.14
2.5 Thermal Effects on Tank Waste Chemistry	2.14
2.6 Mixture of Sludge, Supernate, and Pure Water	2.17
2.7 Mixture of Sludge and Supernate at 25° for Case II	2.20
2.8 Thermal Effects on Tank Waste Chemistry for Case II	2.21
2.9 Mixture of the Sludge, Supernate, and Pure Water for Case II	2.23
3.0 Transport Behavior	3.1
3.1 CSTS Transport Criteria	3.1
3.2 Specie Specific Rheological Behavior	3.2
3.2.1 Aluminum	3.2
3.2.2 Iron Hydroxides	3.3
3.2.3 Phosphates	3.3

3.3	Settled Slurry Volume Fraction and Sedimentation Behavior	3.3
3.4	Waste Property and Transport Behavior Estimates	3.4
3.4.1.	Rheology of the Waste Mixtures	3.4
3.4.2	Predictions of the Energy Required for Waste Transport	3.6
3.4.3	Slurry Transport Evaluations	3.10
3.4.4	Results of the Transport Behavior Predictions	3.13
3.4.5	Predicted Transport Behavior Relative to Acceptance Criteria	3.13
4.0	Summary and Conclusions	4.1
5.0	References	5.1

Figures

2.1 Barney's Aluminum Phase Diagram	2.2
2.2. Predicted Changes of $Al(OH)_4^-$ with OH^-	2.8
2.3 Variations of OH^- with Other Aqueous Species in the Interstitial Solution	2.12
2.4 Predicted Aqueous Species Concentrations with Measured Data	2.13
2.5 Predicted Solid Concentrations with Measured Data	2.13
2.6 Predicted Aqueous Species Concentrations from Mixing SY-102 Sludge and Supernate ..	2.15
2.7 Predicted Solid Concentrations Resulting from SY-102 Sludge/Supernate	2.15
2.8 Predicted Aqueous Species Concentrations Resulting from Mixing Tank SY-102 Sludge and Supernate	2.16
2.9 Predicted Solid Concentrations Resulting from Mixing the Tank SY-102 Sludge and Supernate	2.17
2.10 Predicted Aqueous Species Concentrations Resulting from Mixing the Tank SY-102 Sludge and Supernate with Pure Water at 25°C	2.18
2.11 Predicted Solid Concentrations Resulting from the Tank SY-102 Sludge and Supernate with Pure Water at 25°C	2.18
2.12 Comparison of Predicted Aqueous Species Concentrations with/Without Water	2.19
2.13 Comparison of Solids with and Without Additional Water	2.19
2.14 Predicted Aqueous Species Concentrations Resulting from Mixing the Tank SY-102 Sludge and Supernate at 25°C for Case II	2.20
2.15 Predicted Solid concentrations Resulting from the Tank SY-102 Sludge and Supernate at 25°C for Case II	2.21
2.16 Predicted Aqueous Species Concentrations Resulting from Mixing the Tank SY-102 Sludge and Supernate at 25, 50 and 75°C for Case II	2.22
2.17 Predicted Solid concentrations Resulting from the Tank SY-102 Sludge and Supernate at 25, 50 and 75°C for Case II	2.22
2.18 Predicted Aqueous Species Concentrations from the Mixture of Tank SY-102 Sludge and Supernate with Pure Water at 25°C for Case II	2.23
2.19 Predicted Solid Concentrations Resulting from the Mixture of Tank SY-102 Sludge and Supernate with Pure Water at 25°C for Case II	2.24

Tables

2.1	Constants for the Phosphate Solubility Model of Reynolds (1987)	2.3
2.2	Chemical Compositions and Their Concentrations for Interstitial Solution	2.6
2.3	Chemical Compositions and Their Concentrations for Solids	2.7
2.4	Summary of Solid Testing by GMIN	2.11
2.5	Measured Aqueous Species Concentrations in the Supernate	2.14
3.1	Slurry Acceptance Criteria Based on the CSTS Function Design Criteria	3.1
3.2	Summary of Slurry Transport Cases	3.4
3.3	Coefficients for Equation 3.1	3.5
3.4	Summary of Estimates for Case I	3.11
3.5	Summary of Estimates for Case II	3.12

1.0 Introduction

Hanford Tank 241-SY-102 (SY-102) is currently the only active-service double-shell tank (DST) in the 200 West area. It continues to receive waste from a number of sources within the area, most recently salt well liquors from the 241-S farm through the doubly contained receiver tank (DCRT) 244-S^(a). A summary of available tank characterization data acquired before these more recent transfers is given by DiCenso et al. (1995), who report that the tank currently contains approximately 470 kL (125 kgal) of sludge wastes from a variety of sources including the Plutonium Finishing Plant, T-Plant, and the 222-S Laboratory. In addition, approximately twice this amount (about 930 kL) of dilute, noncomplexed waste forms a supernatant liquid layer above the sludge.^(a) This supernatant layer contains the liquid that remained after the cross-site transfer from 241-SY-102 to 241-AP-104 earlier this year.

With much of the remaining waste in Tank 241-SY-102 scheduled for retrieval in 1996, efforts are under way to establish a technical basis for mobilization of the slurry, waste retrieval, and slurry transport. Because the planned transfer of this waste will use the new Cross-Site Transfer System (CSTS), the slurry that results from the mobilization and retrieval operations must meet the applicable waste acceptance criteria for this system.

In preparation for this effort, analyses are being performed to determine the potential for Tank SY-102 waste properties being adversely affected by mixing the current tank contents or injecting additional diluent into the tank during sludge mobilization. As a part of this effort, the effects of waste heating that will occur as a result of mixer pump operations are also examined. Finally, the predicted transport behavior of the resulting slurries is compared with the waste acceptance criteria for the CSTS.

These analyses are planned to occur in two phases: first, a general, preliminary assessment is made of the technical issues related to heating, diluent choice, and resulting transport behavior; the second phase, if necessary, will explore in more detail technical issues that remain unresolved from the first phase. This report describes the results of the preliminary assessment regarding chemical reactions, rheology, and predicted transport behavior by assuming that the wastes and diluent are fully mixed throughout the tank. Thus the tank was treated as a fully mixed beaker under the preliminary assessment. Under this simplified condition, we determined potential chemical reactions and associated rheology changes to evaluate the feasibility of Tank SY-102 waste retrieval. We also examined approximate ranges of design and operational conditions and their potential impact on waste properties. For the preliminary assessment on chemical reactions, we applied the equilibrium chemical code GMIN (Felmy 1990) to uniformly mixed conditions at various temperatures.

Throughout this assessment we have assumed that the information provided in the Tank Characterization Report for Tank 241-SY-102 by DiCenso et al. (1995) is accurate and complete. Due to the relatively short time available for this effort, we did not generally refer to any of the original documents. Therefore, we do not confirm or deny any of the information in DiCenso et al., except to point out potential inconsistencies.

(a) Sutey, M. J. September 20, 1995. *Waste Compatibility Assessment of Tank 241-SY-101, 103, 106, 107, 108, 109, 110 with Tank 241-SY-102 Waste via DCRT 244-S*. Draft Internal Memo 77240-95-030 to S. H. Rifaey, WHC, Richland, Washington.

2.0 Tank Waste Chemistry

Hanford Tank 241-SY-102 continues to receive waste from a number of sources within the 200 West area. Analyses are being performed to assess potential problems that may occur during the planned transfer of this waste using the new Cross-Site Transfer System (CSTS). To this end, waste properties related to the waste chemistry and transport behavior have been reviewed, and a preliminary assessment has been made of the effects of waste mixing, the addition of diluent, and the transport behavior of the resulting slurries and how they compare with established waste acceptance criteria for the CSTS.

2.1 Background

2.1.1 Aluminum Phases

The chemistry and behavior of aluminum has been the subject of numerous investigations, including those on defense-related production processes, radioactive waste management, and many industrial processes. Because aluminum is a major constituent in the sludge of SY-102 and often plays an important role in determining transport properties, we attempt here to ascertain the particular phases present in this waste. Later, we use an equilibrium chemistry model to predict the relative abundance of aluminum in the solid and liquid phases. This information will help determine whether the resulting slurries will meet the applicable waste acceptance criteria for the transport system.

Barney (1976) was the first to demonstrate the effect of high ionic strength (typical of most defense-related waste streams) on the solubility of aluminum. The aluminum solubility limits indicated by Barney's experimental measurements (obtained with solutions saturated with sodium nitrate, sodium nitrite, sodium carbonate, and sodium sulfate) are given in Figure 2.1. The solubility limits for the pure water system reported by Vol'f and Kuznetsov (1955) (as given in Barney 1976) are shown as dashed lines in the figure. From this information, it is clear that the solubility of aluminum hydroxides is greatly increased at higher ionic strengths, so that for solutions with high sodium hydroxide concentration (above 2 M), increasing aluminum concentration will eventually precipitate sodium aluminate salts that have been commonly observed during evaporator campaigns and were recently observed in samples from Tank 241-SY-101 (Liu et al. 1995b).

At lower sodium hydroxide levels, increases in the molar aluminum concentration eventually results in precipitation of aluminum hydroxides. These aluminum hydroxides may take on several forms, including amorphous, gibbsite, and boehmite. The amorphous form is thought to precipitate out the most quickly, sometimes forming gels that can be particularly problematic during waste transport. The amorphous hydroxide is usually converted in hours or days into a crystalline gibbsite phase. Gibbsite typically forms roughly spherical-shaped primary particles that are of colloidal size (i.e., less than 1 μm) but has been observed in waste streams as a stable agglomerate that is typically between 10 and 100 μm (see, for example, Bunker et al. 1995a). Gibbsite is thought to be relatively common among the waste aluminum phases and has been observed recently in samples from Tank 241-SY-103 (Liu et al. 1995b).

Although boehmite is the thermodynamically favored phase, it is thought to be less common in the waste, occurring only where ample energy has been available over long time periods. Perhaps the most common situation in which this has been true in the tank farms is where some of the waste "self-boiled" for a period due to high decay heat. Boehmite has been observed in one of the tanks (Tank 241-T-111) where self-boiling occurred (Liu et al. 1995a).

From the analyte concentrations given in DiCenso et al. (1995), the total aluminum concentration in the mixed slurry will be approximately 2.3 M, and the sodium hydroxide concentration will be near or below 0.5 M. This puts the 102-SY slurry well within the region where aluminum

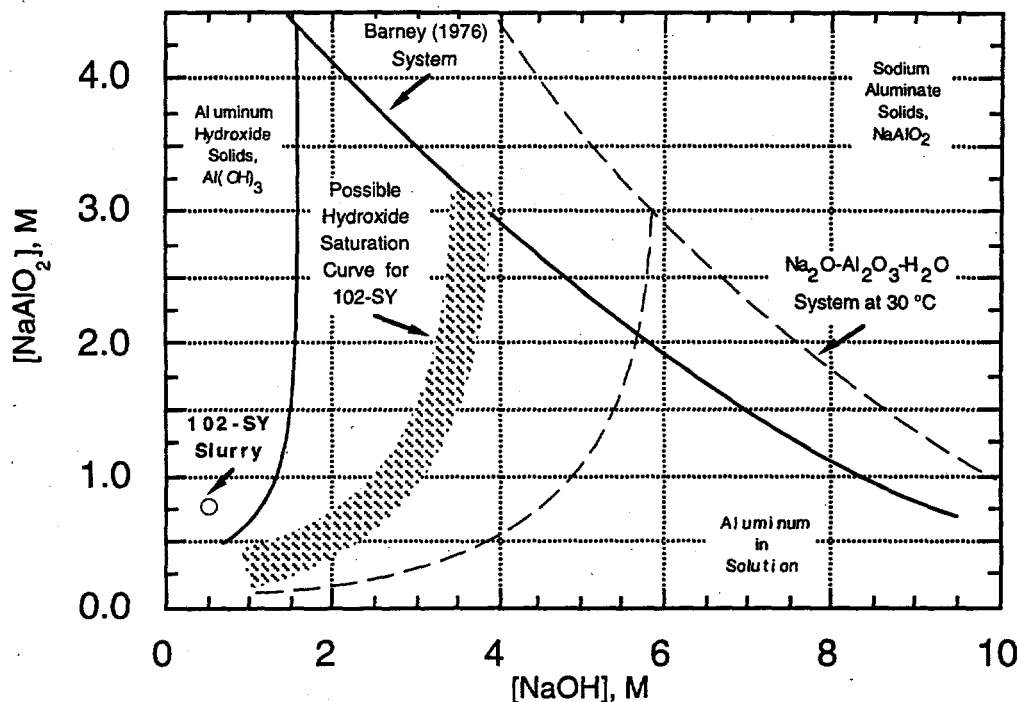


Figure 2.1. Barney's Aluminum Phase Diagram (adapted from Barney [1976]) (the location of the hydroxide saturation curve for SY-102 [shown as a broad, hashed line] is for example only; its exact location is unknown)

hydroxide solids are expected according to the map of Barney (1976). In addition, the solubility curve for the 102-SY slurry is expected to be shifted to higher sodium hydroxide concentrations, because the salts in Barney's system are below saturation in the slurry resulting from 102-SY mobilization. Therefore, the sodium hydroxide solubility curve for 102-SY is located between that of the Barney system and that of the water-aluminum system (see Figure 2.1).

2.1.2 Phosphates

The presence of phosphate salts in the solid phase of the waste can also present challenges during waste transport operations. For this reason, the solubility of phosphates in Hanford waste streams has been the topic of several investigations.

For example, Herting (1987) provides data on phosphate solubility from experimental measurements on simulated defense waste. These data describe phosphate solubility as a function of temperature and sodium concentrations. Because the number of waters of hydration also vary with temperature and sodium concentration, Herting also provides a description and a phase regime map of the morphology of the solids that precipitate. According to this information, phosphate salts precipitate at low sodium concentration (below 5 M) as prisms, or pencil shaped solids. At moderate sodium concentrations (roughly $5 < [\text{Na}] < 10$ M, depending on temperature), the precipitate is a needle-shaped (high aspect ratio) crystal. The solids that were precipitated from solutions with sodium concentrations above 10 M were described as "chunks."

Reynolds (1987) used the data of Herting (1987) to develop a predictive equation for phosphate solubility. The equation had the form

$$[\text{PO}_4] = A/[\text{Na}]^3 + B/[\text{Na}]^2 + C/[\text{Na}] + D \quad (2.1)$$

where each of the coefficients A, B, C and D were parabolic fits of temperature. For example,

$$A = a_0 + a_1 T + a_2 T^2 \quad (2.2)$$

The constants for this model were tabulated by Reynolds and are presented in Table 2.1.

The tank inventory estimate for phosphates given by DiCenso et al. (1995) is 16,400 kg. If we assume that the current total waste height in Tank 241-SY-102 is 3.4 m (135 in.), then the waste volume is approximately 1,225,000 L (322,600 gal) and the average phosphate concentration is

$$[\text{PO}_4] = \frac{16,400 \text{ kg} \left(1000 \frac{\text{g}}{\text{kg}} \right) \left(\frac{\text{g moles}}{94.97 \text{ g}} \right)}{1,225,000 \text{ L}} = 0.14 \text{ M} \quad (2.3)$$

Although the data of Herting do not include temperatures as low as 25°C or sodium concentrations as low as some of the cases considered in this study, the solubility model of Reynolds (1987) may be extrapolated to the worst case we consider (that of high sodium concentration, low temperature, and no water addition, later referred to as Case II-A at 25°C). In this case the sodium concentration is approximately 5.1 M at 25°C, and an extrapolated prediction from Reynolds model gives 0.10 M as the solubility limit. Thus in this case the some phosphate solids might be present, but only in small concentrations. If the concentration of solid phase phosphates is 0.14 - 0.10 = 0.04 M, then these solids represent less than 0.4 wt% of the solution. This small amount will not significantly affect the transport behavior.

For all the other cases considered in this effort, the solubility of phosphates is predicted to be well above the waste concentration so that all of the phosphates are expected to be in solution. For example, in the case of high sodium concentration at 50°C (referred to later as Case II-A at 50°C), the sodium concentration is 4.2 M and the predicted phosphate solubility is 0.77 M, well above the 0.14 M present in 102-SY.

For these reasons, we will generally assume that the phosphates present in Tank 241-SY-102 are in solution and thus will not affect transport behavior. We will, however, briefly consider how phosphate solubility can be modeled with the equilibrium chemistry model later in this section.

Table 2.1. Constants for the Phosphate Solubility Model of Reynolds (1987)

	a_i	b_i	c_i	d_i
0	-5181.902	2656.08	-425.7586	20.71154
1	180.5396	-95.25732	15.53686	-0.7619675
2	-1.219804	0.697907	-0.1187975	6.032556E-03

2.1.3 Iron, Lead, and Manganese

Iron, lead, and manganese are assumed to be insoluble in the waste solutions. From the constituent concentrations provided in DiCenso et al. (1995), the solid fraction of the 102-SY waste contains approximately 4.7 wt% iron hydroxide ($\text{Fe}(\text{OH})_3$) if this is assumed to be the only iron specie present. Lead and manganese hydroxides account for less than 2 wt% of the solid phase. Therefore, in the present effort we assume that a total of 7 wt% of the solid phase consists of these and any other "insoluble" constituents.

2.2 Chemical Modeling Approach

DiCenso et al. (1995) report that supernatant liquid chemical composition is significantly different from that of the interstitial solution, implying that the supernatant liquid is not in an equilibrium condition with solids in the sludge. Thus, to simulate the potential chemical reactions of the tank waste with diluent at different temperatures, we assumed that the interstitial solution of the sludge is in equilibrium with the solids of the sludge. We assumed the measured aqueous species concentrations of the interstitial solution in the sludge to be correct and used them as a starting point for the modeling. Thus the following steps were taken to simulate chemical reactions for the various cases:

- STEP 1. Assign cations, anions, and neutral aqueous species with correct charge balance for the interstitial solution of the sludge by using the measured analytical chemistry data. The final selection of all aqueous species was performed iteratively between Step 1 and Substeps 2.1 and 2.2.
- STEP 2. Determine solids in the sludge that are saturated with the interstitial solution.
- Substep 2.1. Simulate chemical reactions between interstitial solution and one solid at a time to determine which solids are in saturation with the measured interstitial solution without much change in solution chemistry.
- Substep 2.2. Simulate chemical reactions of aqueous species and all solids (selected under Substep 2.1) together to confirm that these solids are saturated with the interstitial solution without much change in solution conditions.
- Substep 2.3. Increase amount of solids to match to the amount reported in DiCenso et al. (1995) without changing solution chemistry.
- STEP 3. Simulate chemical reactions under full mixture of sludge (both the interstitial solution and solids as selected under Step 2) and the supernate at 25°C. The volume ratio of the supernatant and sludge was selected to be 2:1.
- STEP 4. Simulate chemical reactions under full mixture of sludge and the supernate at temperature of 50 and 75°C and higher (if appropriate). These cases represent conditions of tank waste heating due to the mixer pump operation.
- STEP 5. Simulate chemical reactions under full mixture of sludge, the supernate, and pure water at temperature of 25°C. This case represents additional diluent added to Tank SY-102. We selected the additional diluent to be 930,000 kL of pure water. Thus the volume ratios of the pure water:the supernate:the sludge are 2:2:1.

We used the chemical model GMIN to simulate chemical reactions and phase equilibria. The GMIN code calculates the chemical composition of systems composed of aqueous phases, pure solid

phases, solid-solution phases, adsorbed phases, and gas phases. In the aqueous phase modeling, the excess solution free energy is modeled by using the Pitzer equations (Harvie et al. 1987), which are valid to high ionic strengths. Thus, GMIN is applicable to tank waste conditions having high ionic strength. The Davies equations (Felmy 1990) can also be used as an option in the GMIN code. The mathematical algorithm in GMIN is based on a constrained minimization of the Gibbs free energy (Snoeyink and Jenkins 1980; Harvie et al. 1987). This approach is more numerically stable and reliably converges to a free energy minimum, compared with more common chemical equilibrium codes based on the mass-action approach (Felmy 1990). In GMIN, the activity coefficients for non-ideal, solid-solution phases are calculated using parameters of a polynomial expansion in mole fraction of the excess free energy of mixing. The free energy of adsorbed phase species is described by the triple-layer, site-binding adsorption model. For this study, we used the Pitzer equation.

2.3 Chemistry Of Sludge

2.3.1 Aqueous and Solid Species Measurements

Tank SY-102 contains 466,000 L (123,000 gal.) of sludge weighing 727,000 kg (16,000,000 lb), and approximately 932,000 L (246,000 gal.) of supernatant liquid weighing 960,000 kg (2,110,000 lb) (DiCenso et al., 1995). The sludge consists of 440,000 kg of solids and 287,000 kg of interstitial solution. The sludge contains Al, Ca, Cr, Fe, Pb, K, Mn, Na, Cl, Si, N, P, S, inorganic carbon, and organic carbon.

Based on the characterization report by DiCenso et al. (1995), we selected the following species for the interstitial solution to perform the chemical reaction modeling: Al(OH)_4^- , Ca^+ , Cr(OH)_4^- , K^+ , Na^+ , CO_3^{2-} , Cl^- , $\text{H}_2\text{SiO}_4^{2-}$, NO_3^- , NO_2^- , PO_4^{3-} , SO_4^{2-} , and F^- . For interstitial solution, aqueous species selected in this study and their measured or estimated molalities are presented in Table 2.2, based on the description of the tank sludge by DiCenso et al. (1995). These molality values were input into GMIN for the sludge.

DiCenso et al. (1995) do not report a hydroxide concentration for the interstitial solution when the species listed in the table are assumed, and the charge balance between measured cations and anions was off by 2.689. Since the carbonate concentration was not measured for the interstitial solution, we assigned difference between their concentrations in bulk sludge and solids as its concentration in the solution. As we discussed in Section 2.2.1, the hydroxide is a critical aqueous specie for determining solubilities of at least $\text{NaNO}_3(\text{s})$, $\text{NaNO}_2(\text{s})$, and aluminum solids, such as gibbsite and sodium aluminate. Thus the lack of hydroxide data causes some uncertainty in that study.

For the solids in the sludge, we selected these chemical forms to be included in the chemical modeling: $\text{Al(OH)}_3(\text{s})$, $\text{CaCO}_3(\text{s})$, amorphous Cr(OH)_3 , sylvite, thermonatrite, $\text{NaNO}_3(\text{s})$, $\text{NaNO}_2(\text{s})$, halite, $\text{Na}_3\text{PO}_4 \cdot 12\text{H}_2\text{O}$, and thenardite, $\text{NaF}(\text{s})$. The following solids and their estimated molalities are presented in Table 2.3, again based on the DiCenso et al. (1995) description. Fe, Mn, and Pb are not included in the modeling because GMIN does not have a thermodynamic database for the relevant species. Thus, as per the earlier discussion, we treated them as "insoluble" solids. Since aqueous concentrations of Fe and Mn species in the interstitial solution are quite low, this assumption was judged to be reasonable and conservative for the waste transport analysis that follows.

2.3.2 Aqueous Species Selection (Step 1)

DiCenso et al (1995) reported concentrations of aqueous species in the interstitial solution of the sludge, as shown in Table 2.2. These were included in our modeling. However, the total charge of cation species reported is 9.584, while the total charge of anions is 6.895; thus there is an imbalance of 2.689. Since the hydroxide was not measured in their analysis, its concentration can be

Table 2.2. Chemical Compositions and Their Concentrations for Interstitial Solution

Compound	Measured Concentration $\mu\text{g/g}$	Aqueous Species	Measured or Estimated Concentration ($\mu\text{g/g}$)	Molality
Al	3,100	Al(OH)_4^-	10,916*	0.29090
Ca	44	Ca^+	44	0.00279
Cr	565	Cr(OH)_4^-	1,301*	0.02740
K	2,350	K^+	2,350	0.15220
Na	85,600	Na^+	85,600	9.42600
TIC	16	CO_3^{2-}	80	0.00337
Cl		Cl^-	2,540	0.18140
Si	218	$\text{H}_2\text{SiO}_4^{2-}$	270*	0.00726
		NO_3^-	94,900	3.87500
		NO_2^-	31,600	1.73900
P	1,580	PO_4^{3-}	4,750	0.12660
S		SO_4^{2-}	6,270	0.16520
F		F^-	373	0.04971

* Denotes its concentration was estimated by assigning associated aqueous species in this study.

as high as 2.689 molality. As we discuss later in this report, we simulated chemical reactions with various molalities of hydroxide concentrations to select its value best fit to the overall chemical reaction conditions occurring between interstitial solution and solids within the sludge.

2.3.3 Selection of Appropriate Solids (Substep 2.1)

For a specific solid to be present in the sludge, the interstitial solution must be saturated with that solid, i.e., it must be a solubility-controlling solid. We identified 15 solids: $\text{Al(OH)}_3(\text{s})$, calcite, gypsum, amorphous Cr(OH)_3 , sylvite, thenardite, $\text{NaNO}_3(\text{s})$, $\text{NaNO}_2(\text{s})$, $\text{Na}_3\text{PO}_4 \cdot 12\text{H}_2\text{O}$, amorphous SiO_2 , $\text{Na}_3\text{PO}_4 \cdot 10\text{H}_2\text{O}$, $\text{Na}_3\text{PO}_4 \cdot 8\text{H}_2\text{O}$, thenardite, $\text{NaF}(\text{s})$, and halite) as potential candidates as solubility controlling solids for the interstitial solution. To determine which solids are actually controlling solids, GMIN simulated equilibrium chemical reactions between interstitial solution and these 15 solids with one solid as a time. Following is the summary of these simulation results.



We ran the GMIN code with only gibbsite present as a solid to examine if the interstitial solution is saturated with gibbsite. Since there was no measured hydroxide concentration available for the interstitial solution, we assigned its concentration to be 0.5, 1.0, 1.5, 2.0 and 2.689 m in solution. The carbonate concentration was then assigned to be 1.0962, 0.8480, 0.5980, 0.3480, and 0.0338 m, respectively. The sum of the hydroxide and carbonate charges is 2.8480, matching the imbalance between the positive and negative charges reported in DiCenso et al. (1995). As we stated

Table 2.3. Chemical Compositions and Their Concentrations for Solids

Compound	Measured Concentration $\mu\text{g/g}$	Assumed Solid Species	Estimated Concentration $\mu\text{g/g}$	Molality
Al	45,600	$\text{Al(OH)}_3(\text{s})$	131,800	6.5600
Ca	11,500	$\text{CaCO}_3(\text{s})$	28,720	1.1140
Cr	18,900	$\text{Cr(OH)}_3\text{am}$	37,450	1.4110
Fe	40,900			
Mn	10,900			
K	3,340	sylvite	6,368	0.2162
Na	140,000			
CO_3	6,400			
		thermonatrite	8,354	0.1995
NO_3	64,300	$\text{NaNO}_3(\text{s})$	88,140	4.1220
NO_2	14,400	$\text{NaNO}_2(\text{s})$	21,600	1.2150
PO_4	34,000	$\text{Na}_3\text{PO}_4 \cdot 12\text{H}_2\text{O}$	136,000	1.3900
SO_4	4,300	thenardite	6,370	0.1741
F	3,180	$\text{NaF}(\text{s})$	7,028	0.6497
Cl	1,310	halite	2,160	0.1435

previously, the carbonate concentration was indirectly obtained to be 0.0338 m by measured carbonate concentrations in the bulk sludge and solid portion of the sludge.

GMIN indicated that in all these cases with different hydroxide concentrations, the solution is saturated with gibbsite. The simulation results varied from slight gibbsite precipitation (0.196 m) for the 0.5 m hydroxide concentration case to slightly dissolving (0.055 m) for the hydroxide concentration of 2.689 m case. Thus we concluded that gibbsite is present in the solid.

Predicted Al(OH)_4^- concentrations are 0.0945, 0.1530, 0.2110, 0.2688, and 0.3450 m with resulting hydroxide concentrations of 0.725, 1.165, 1.607, 2.049, and 2.6620 m, respectively, as shown in Figure 2.2.

Estimated Al(OH)_4^- and OH^- concentrations based on DiCenso et al (1995) data are 0.291 and 0.00337 m, respectively (see Table 2.2). As we will discuss in detail, the selection of hydroxide concentrations of 2.689 m provide the best fit for overall aqueous species concentrations. Thus we selected hydroxide and carbonate concentrations to be 2.689 and 0.00338 m, respectively. Unless stated otherwise, the rest of the predicted concentrations described in this report are based on these concentrations as initial concentrations for the chemical modeling.

We also tested these cases by adding $\text{Al(OH)}_3(\text{aq})$ as another potential aqueous species present. The addition of $\text{Al(OH)}_3(\text{aq})$ did not change the prediction results, because GMIN predicted that most of the Al is in Al(OH)_4^- form in the solution at least with temperature below 90°C. At 95°C

Variation of Al(OH)_4^- with OH^-

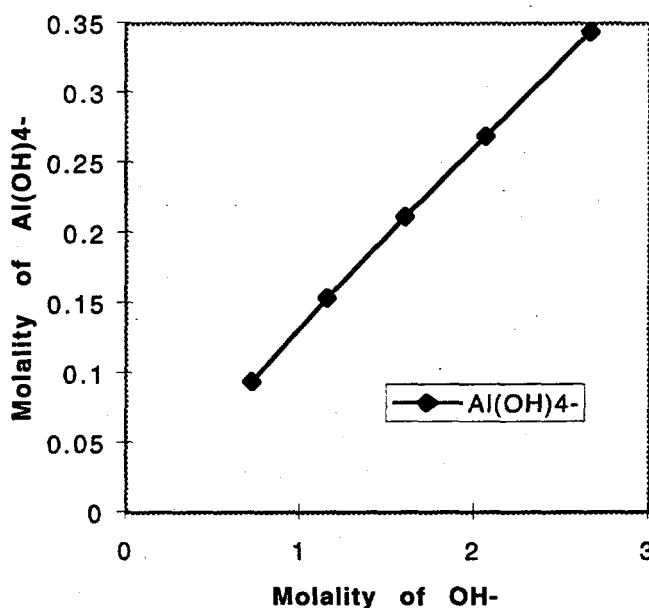


Figure 2.2. Predicted Changes of Al(OH)_4^- with OH^-

and above, the inclusion of $\text{Al(OH)}_3(\text{aq})$ significantly increased gibbsite solubility, resulting in all gibbsite in the sludge dissolving out when the sludge mixed with the supernate. However, there is a large uncertainty in this prediction, and we did not investigate the validity of this prediction further at these high temperatures.



Next we examined whether sodium phosphate is present in the solid as one of the following solid forms: $\text{Na}_3\text{PO}_4 \cdot 12\text{H}_2\text{O}(\text{s})$, $\text{Na}_3\text{PO}_4 \cdot 10\text{H}_2\text{O}(\text{s})$, or $\text{Na}_3\text{PO}_4 \cdot 8\text{H}_2\text{O}(\text{s})$. If sodium phosphate is present in the solid at 25°C, it is most likely in the form of $\text{Na}_3\text{PO}_4 \cdot 12\text{H}_2\text{O}(\text{s})$. We imposed these three solids (one at a time) to be present in the sludge with the interstitial solution. GMIN predicted that the interstitial solutions significantly under-saturated with any of these sodium phosphate solids by much more than 16 m. Thus, although DiCenso et al. (1995) reported that phosphorus was measured in solid (26,800 μg of phosphorus per g of total solids), we concluded that, based on the interstitial solution conditions reported by DiCenso, sodium phosphate is not present among the solids. This is consistent with the discussion in Section 2.1.2. Therefore, phosphates were assumed for the remainder of this study to be contained within the aqueous phase. (Actually, phosphate was also removed from the liquid phase portion of the model due to matrix interference problems.)



When $\text{NaNO}_3(\text{s})$ was assigned as the only solid to react with the interstitial solution, GMIN predicted that 1.756 m $\text{NaNO}_3(\text{s})$ is dissolved for the solution to reach the solubility limit, resulting in small increases of total NO_3^- and Na^+ aqueous concentrations from measured values of 3.875 and 9.046 m to 5.632 and 10.805 m, respectively (with a hydroxide concentration higher than 2.689 m

these values would come down, as GMIN indicated.) Since there are some uncertainties in the model and data accuracy, and a very strong indication that $\text{NaNO}_3(s)$ is present in the solids, we considered that GMIN predicted that the solution is essentially at the solubility limit with $\text{NaNO}_3(s)$ and selected $\text{NaNO}_3(s)$ to be among the solids.

NaNO₂(s)

Next we imposed $\text{NaNO}_2(s)$ as a solid. GMIN predicted a solubility limit for $\text{NaNO}_2(s)$ of about 7 m, indicating the solution is significantly under-saturated with $\text{NaNO}_2(s)$. With approximately 7.4 m of $\text{NaNO}_2(s)$ dissolving, the resulting Na^+ and NO_2^- concentrations in the solution differ from measured values of 9.05 and 1.74 m and are predicted to be 16.44 and 9.123 m, respectively. Although DiCenso et al. (1995) reported that there is 14,400 $\mu\text{g NO}_2^-$ per g of total solid in the sludge, our modeling results with measured interstitial solution as model input strongly imply that $\text{NaNO}_2(s)$ is too much under saturation to be present among the solids. So we eliminated $\text{NaNO}_2(s)$ among the solids in the sludge. This discrepancy of whether $\text{NaNO}_2(s)$ is present may be resolved once solid measurements identify what specific solids are present in the solids.

NaF(s)

When $\text{NaF}(s)$ was imposed to the solution, only 0.065 m of $\text{NaF}(s)$ was dissolved to reach a solubility limit; thus $\text{NaF}(s)$ is judged to be present in the solids.

Thenardite, Na₂SO₄(s)

We imposed thenardite as a sodium sulphate solid to be potentially present in the solids. GMIN predicted that only 0.93 m must be dissolved for the solution to reach its solubility limit with thenardite; so we determined that thenardite exists among the solids in the sludge.

Calcite, CaCO₃(s)

GMIN predicted that the interstitial solution is at the solubility limit with calcite. When only calcite was present as a solid, the model predicted that only 0.005 m of calcite was dissolved to reach the solubility limit. Thus calcite was selected to be present among the sludge solids.

Gypsum, CaSO₄(s)

When gypsum was imposed to the interstitial solution as the only solid present, GMIN predicted that 1.508 m of gypsum was dissolved for the solution to reach a solubility limit with gypsum. Thus, with model and data uncertainty, gypsum can be present (above saturation) or not present (under saturation) among the solids by this simulation alone. However, resulting predicted molalities of Ca^+ (1.433 m) and SO_4^- (1.587 m) were much higher than measured values of 0.00279 m and 0.165 m, respectively. Furthermore, as we discuss later when we impose all selected solids to be present together to examine the validity of our solid selection (Substep 2.3), elimination of gypsum produced better overall matching between the measured and predicted interstitial aqueous species concentrations than the case with gypsum. Thus, we eliminated gypsum from consideration.

Cr(OH)₃am

With only amorphous Cr(OH)_3 present as a solid, GMIN predicted that the interstitial solution is saturated with this solid. The solid was very slightly precipitated (0.027 m). The calculated concentration of hydroxide was slightly changed from 2.689 m to 2.716 m, suggesting that amorphous Cr(OH)_3 is present in the solids.

Themonatrite, Na₂CO₃·H₂O(s)

When themonatrite was assigned as a sole solid, 2.419 m was dissolved for the solution to reach its solubility limit. Correspondingly, Na⁺ and CO₃²⁻ concentrations changed from measured values of 9.046, 2.3216 m to 13.307 and 2.316 m, respectively. The molality of hydroxide was changed from 2.689 m to 2.577 m. Although themonatrite could be judged to be among solids with these results, the GMIN results are more indicative of themonatrite not present among the solids. Thus we eliminated this solid from the list of solids present in the sludge. There are some possibilities that around 25 to 40°C, Na₂CO₃·10H₂O(s) and Na₂CO₃·7H₂O(s) could be present, but we could not examine these possibilities under this preliminary assessment, because this requires first incorporating the associated thermodynamic data into GMIN's database.

Halite, NaCl(s)

To reach the solubility limit with halite, 2.83 m of halite was dissolved, indicating the solution is somewhat under saturation. Consequently both Na⁺ and Cl⁻ in the interstitial solution was increased by 2.83 m. This is a rather significant increase for Cl from 0.181 to 3.012 m. But, as will be discussed later, the inclusion of halite improved the overall matching of aqueous species concentrations with the measured data when all the solids are imposed together. So we kept halite as one of the solids existing in the sludge.

Sylvite, KCl(s)

There was 3.66 m of sylvite dissolved to reach a solubility limit., increasing K⁺ and Cl⁻ by the same amount. Furthermore, the inclusion of sylvite did not improve the matching between the measured and predicted aqueous species concentrations when all the selected solids are imposed together. Thus we eliminated sylvite from the solids present in the solids.

SiO₂am

GMIN predicted that 1.32 m of SiO₂am was dissolved for the solution to reach the solubility limit with amorphous SiO₂. while it predicted H₂SiO₄²⁻ to increase from an estimated 0.00726 m to 1.328 m and OH⁻ to decrease from 2.689 to 0.048 m. Thus we eliminated this solid from being present in the sludge.

Table 2.4 summarizes the amounts of solids that are dissolved or precipitated for the interstitial solution to reach solubility limit with each of the 15 solids tested with the GMIN code.

Combined Solid Cases (Substeps 2.2 and 2.3)

After examining 15 potential solubility controlling solids, the following seven solids were judged to be solubility controlling solids for the interstitial solution, thus believed to be present in the sludge: gibbsite, NaNO₃(s), NaF(s), thenardite, calcite, amorphous Cr(OH)₃, and halite (see Table 2.4). We also further examined gypsum and amorphous SiO₂.

Table 2.4. Summary of Solid Testing by GMIN

Solids	Molality Dissolved	Presence Among the Solids
Gibbsite	0.196 (precipitated)	Yes
Na ₃ PO ₄ ·12H ₂ O(s), Na ₃ PO ₄ ·10H ₂ O(s), and Na ₃ PO ₄ ·8H ₂ O(s)	Over 16.0	No
NaNO ₃ (s)	1.756	Yes
NaNO ₂ (s)	7.378	No
NaF(s)	0.065	Yes
Thenardite	0.932	Yes
Calcite	0.005	Yes
Gypsum	1.508	No*
Cr(OH) ₃ am	0.027 (precipitated)	Yes
Themonatrite	2.419	No
Halite	2.831	Yes
Sylvite	3.660	No
SiO ₂ am	1.320	No*

* After testing all solids together at once, they were eliminated to be present

These tests were performed by GMIN by putting all these selected solids together with the interstitial solution to reproduce the measured concentrations of interstitial solution species and solids. Results indicated that including gypsum and amorphous SiO₂ produced greater discrepancies between the measured and predicted concentrations. Thus these two solids were eliminated from further consideration.

We also examined what molality should be imposed for hydroxide, since it was not measured by DiCenso et al. As discussed previously, we ran GMIN with OH⁻ concentrations of 0.5, 1.0, 1.5, 2.0, and 2.689 m in the solution. The carbonate concentration was assigned to be 1.0962, 0.8480, 0.5980, 0.3480, and 0.0338 m, respectively, to impose the charge balance in the interstitial solution. The some of the predicted aqueous species concentrations are shown in Figure 2.3. This figure clearly indicates that hydroxide molality of 2.662 with the corresponding carbonate molality of 0.00366 produced the closest match with the measured aqueous species concentration for the interstitial solution. Thus these values were selected for our study.

As indicated previously, the OH⁻ value of the interstitial solution estimated by the measured bulk sludge and solid is also 0.00366 m. As discussed in Section 2.1, the aluminum hydroxide solubility curve is shifted to higher NaOH concentration relative to the high ionic strength system studied by Barney (1976). Thus we expect mist of the aluminum in the SY-102 systems to appear in

Variations of OH⁻ with Other Species

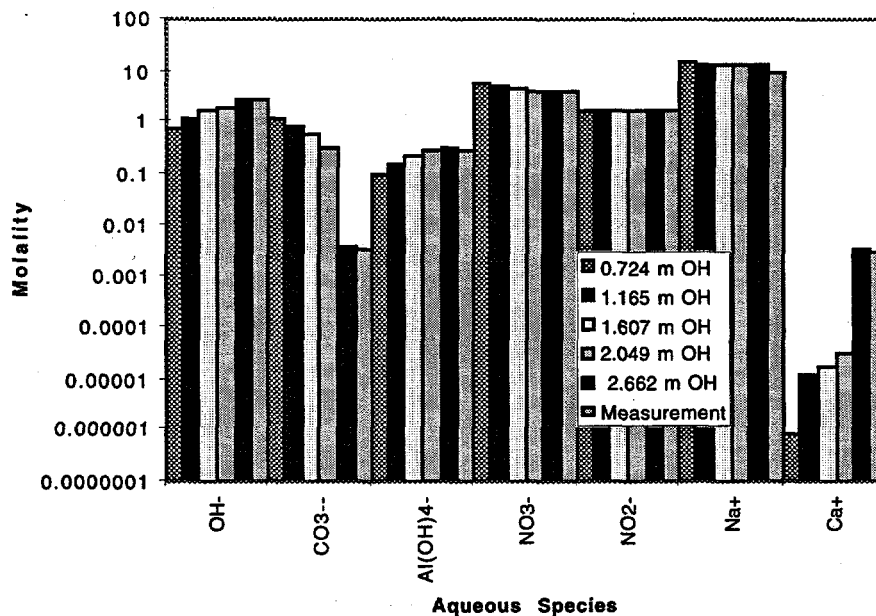


Figure 2.3. Variations of OH⁻ with Other Aqueous Species in the Interstitial Solution

the solid phase as gibbsite. Furthermore, gibbsite has been observed in systems with concentrations of 3 to 10 m NaOH.^(a) Thus our predictions on gibbsite and associated Al(OH)₄⁻ are consistent with this understanding.

The predicted conditions of sludge interstitial solution and solids are presented in Figures 2.4 and 2.5, together with measured data. These figures show that our predictions compare well based on the conditions we imposed (e.g., measured aqueous species concentrations in the interstitial solution were our starting conditions without a priori knowledge of the measured solids present in the sludge).

In the current study, solids containing sodium are NaNO₃(s), thenardite, NaF(s), and halite. These values matched very well with the measured data on these solids, as shown in the figures. However, DiCenso et al. (1995) also reported Na in the solids at concentrations approximately 4.3 times more than that represented by our NaNO₃(s), thenardite, NaF(s), and halite. This large discrepancy may come from the fact that, based on the measured interstitial solution, GMIN predicted no NaNO₂(s), Na₂CO₃(s), or Na₃PO₄(s). Some other sodium-containing solids may also exist that we have not included. Without information on the solid generation, there is no suitable way to reconcile the differences. Thus for this preliminary study, we conducted two separate conditions. Case 1 imposed the amount of sodium-containing solids to be that derived based on the anion measurements on the solids, as reported by DiCenso et al. Case 2 imposed amounts of NaNO₃(s), thenardite, NaF(s), and halite 4.3 times more than Case 1 imposes, so that the reported values of sodium are included. The following results thus cover both Cases 1 and 2. We will first consider the model predictions based on Case 1.

(a) Sterner, S. M., J. R., Rustad, and A. R., Felmy, 1995. *Chemical Modeling for the Major Electrolyte Components of the Hanford Waste Tanks II. ESP Parameters for the System: Na-NO₃-NO₂-CO₃-F-PO₄-OH-H₂O with New Parameters to Include Al(OH)₄⁻ and Cr(OH)₄⁻*. TWRSP-95-018, Pacific Northwest National Laboratory, Richland, Washington.

Sludge Interstitial Solution

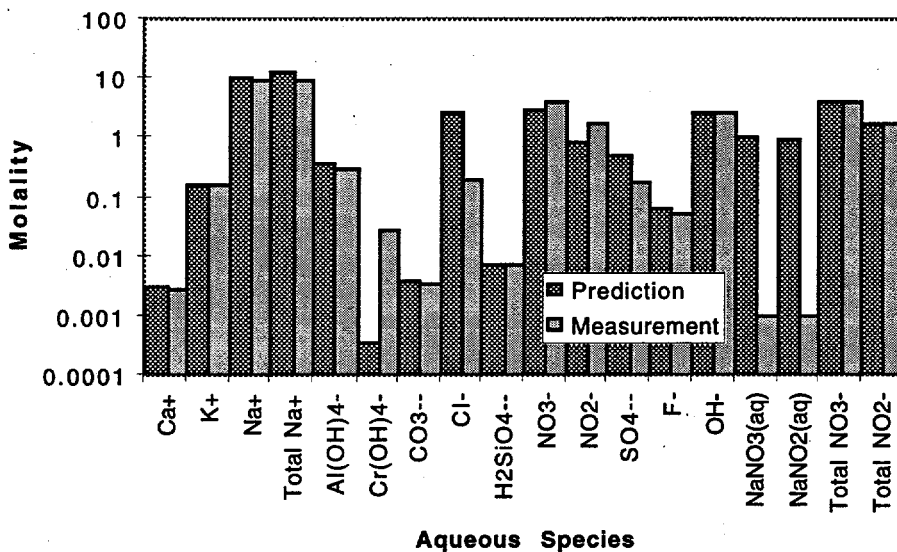


Figure 2.4. Predicted Aqueous Species Concentrations with Measured Data

Solids in Sludge

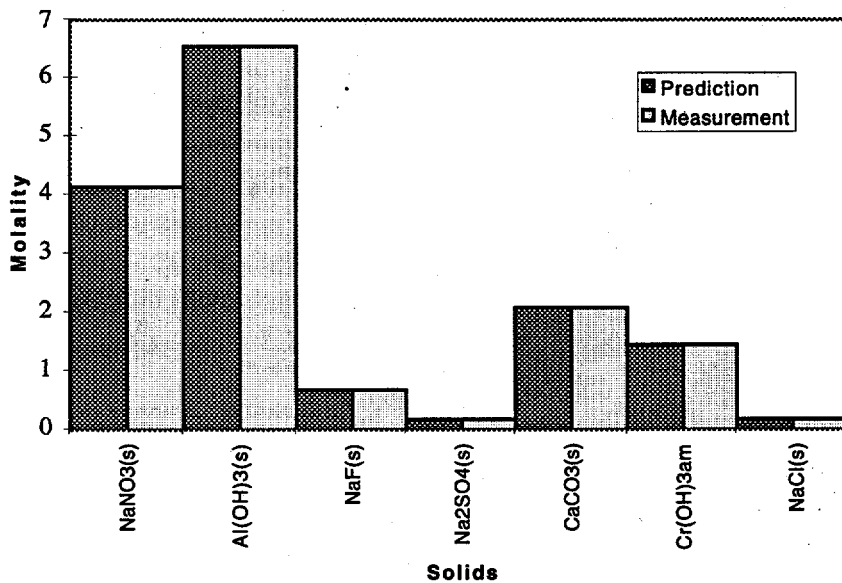


Figure 2.5. Predicted Solid Concentrations with Measured Data

2.4 Mixture of Sludge and Supernate at Temperature 25°C for Case 1

The supernate in Tank SY-102 was assumed to contain 932,000 L (246,000 gal.), twice the volume of the sludge. The density of the supernate was reported to be 1.03 kg/L. Table 2.5 shows the measured aqueous species concentrations of the supernate (Dicenso et al. 1995).

Assuming the sludge and the supernate are fully mixed, GMIN simulated equilibrium chemical reactions at 25°C. The predicted solution chemical composition and solids at this temperature are presented in Figures 2.6 and 2.7, respectively. These figures also show the corresponding solutions and solids if there were no chemical reactions occurring.

As shown in these figures, all Na-containing solids, i.e., NaNO₃(s), thenardite, NaF(s), and halite are dissolved out, and the solution is still under saturated with them (see Figure 2.7 for the comparison with and without chemical reactions). However, GMIN also predicted that a relatively small amount (0.0188 m) of gibbsite was precipitated at 25°C, while the mixed solution is practically at solubility limits with amorphous Cr(OH)₃ and calcite. Amorphous Cr(OH)₃ precipitated only 0.00007 m, and calcite dissolved 0.001 m, according to GMIN.

Thus, based on the modeling approach we took, the mixing of the sludge and the supernate in Tank SY-102 dissolves all Na-containing solids but does not significantly affect amorphous Cr(OH)₃ and calcite. At the same time a very small amount of gibbsite may precipitate.

2.5 Thermal Effects on Tank Waste Chemistry

We examined the potential effects of temperature on chemical reactions of the mixture of the sludge and supernate above 25°. These temperature rises above 25°C are due to the heat generated by pumps to mix the sludge and supernate. We selected 50 and 75°C for the study.

Table 2.5. Measured Aqueous Species Concentrations in the Supernate (DiCenso et al. 1995)

Compound	Measured Concentration μg/g	Aqueous Species	Measured or Estimated Concentration, μg/g	Molality
Al	617	Al(OH) ₄ ⁻	2,173*	0.02408
Na	16,800	Na ⁺	16,800	0.7692
TIC	<16	CO ₃ ²⁻	<97	<0.001706
Cl		Cl ⁻	194	0.005761
		NO ₃ ⁻	22,800	0.3871
		NO ₂ ⁻	3,130	0.07162
P		PO ₄ ³⁻	385	0.004267
S		SO ₄ ²⁻	506	0.005545
F		F ⁻	730	0.004044
		OH ⁻	3,370	0.2086

* Concentration was estimated by assigning associated aqueous species in this study.

Sludge and Supernate at 25 Degree C

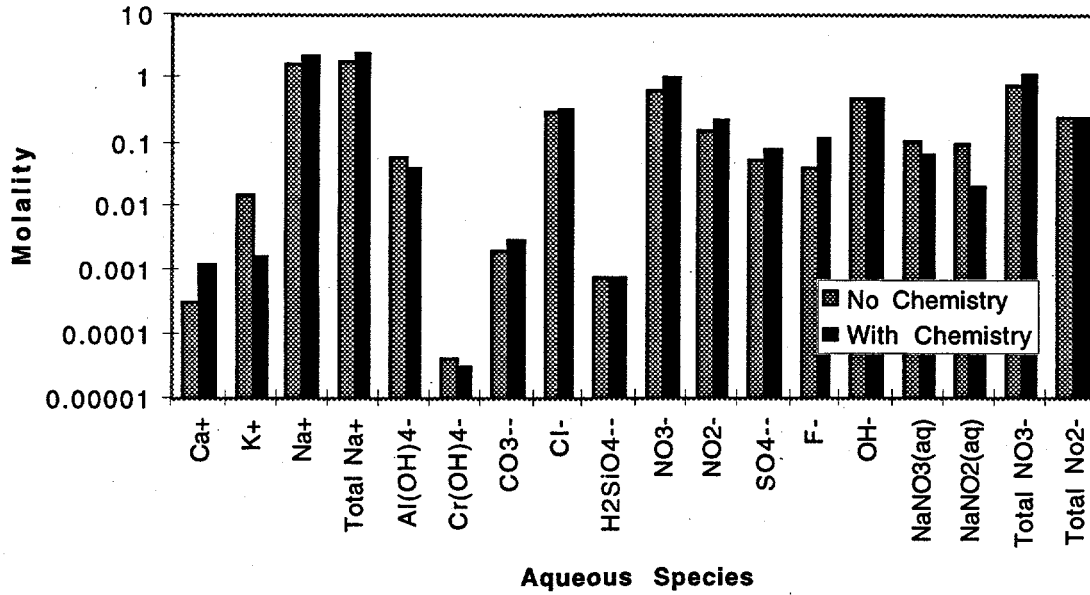


Figure 2.6. Predicted Aqueous Species Concentrations from Mixing SY-102 Sludge and Supernate

Sludge and Supernate at 25 Degree C

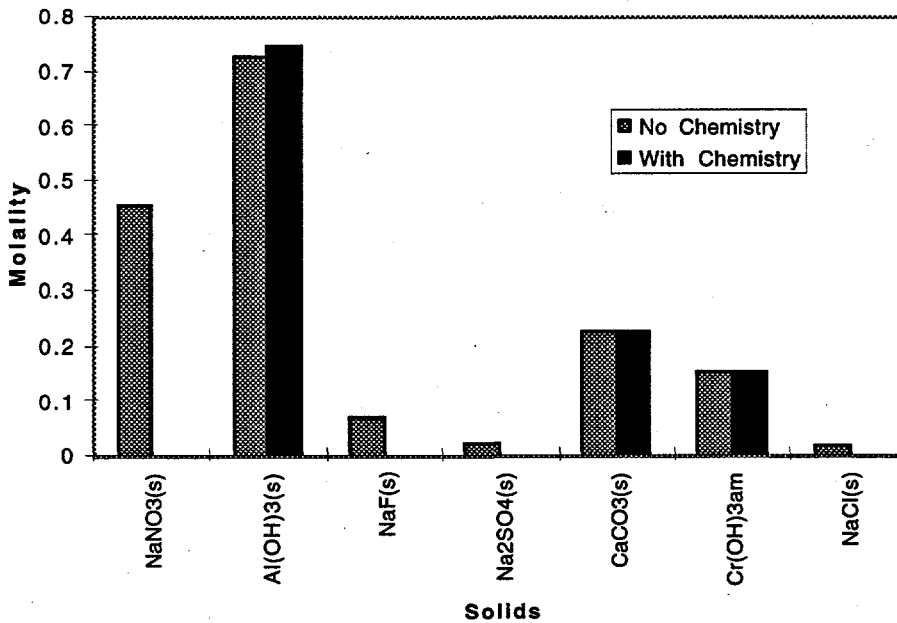


Figure 2.7. Predicted Solid Concentrations Resulting from SY-102 Sludge/Supernate

Similar to the temperature of 25°C, all Na-containing solids of NaNO₃(s), thenardite, NaF(s), and halite are dissolved out at 50 and 75°C. Predicted solutions at 50 and 75°C are presented in Figure 2.8. Corresponding results for the solids are presented in Figure 2.9. These figures also contain the predicted results at 25°C for the comparative purpose.

At 50 and 75°C NaNO₃(s) is even more under saturated than at 25°C, while thenardite, NaF(s), and halite are somewhat less under saturated than at 25°C, according to the model results. This trend was also observed when the temperature was raised to 100°C.

However, unlike at 25°C, due to the increase of gibbsite solubility at higher temperatures, approximately 3 and 13% of the gibbsite in the Tank SY-102 are dissolved into the solution at 50 and 75°C, respectively. The corresponding predicted concentrations of Al(OH)₄⁻ increased from 0.0408 m at 25°C to 0.152 m at 75°C. Note that predicted hydroxide concentrations were slightly lower at these higher temperatures, possibly helping the increase of the gibbsite solubility. The inclusion of Al(OH)₃(aq), as one of the potential aqueous chemical species, did not change the results at 25, 50 and 75°C, but at 100°C, this inclusion significantly increased gibbsite solubility to the point of total dissolution of gibbsite. Without Al(OH)₃(aq), gibbsite solubility at 100°C was higher than the other lower temperatures, but not to the point of dissolving all gibbsite. As shown in Figures 2.8 and 2.9, changes of calcite and amorphous Cr(OH)₃ at 50 and 75°C are minimum.

These model results suggest that at higher temperature, all Na-bearing solids are dissolved. Also gibbsite will not precipitate, while calcite and amorphous Cr(OH)₃ are not significantly affected.

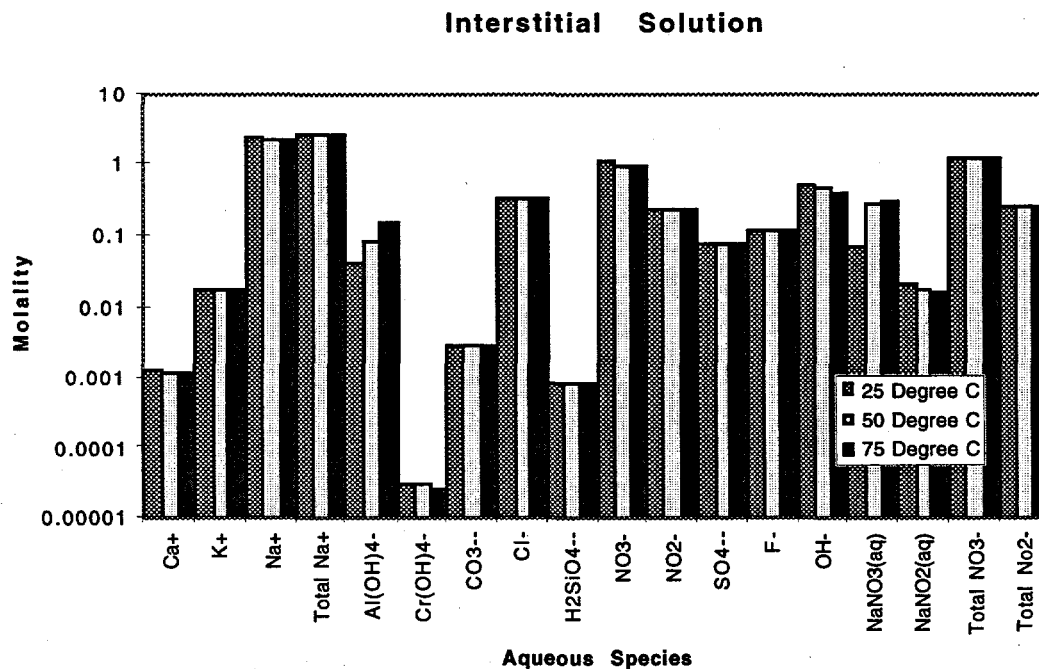


Figure 2.8. Predicted Aqueous Species Concentrations Resulting from Mixing the Tank SY-102 Sludge and Supernate at 25, 50 and 75°C

Solids in Mixture of Sludge and Supernate

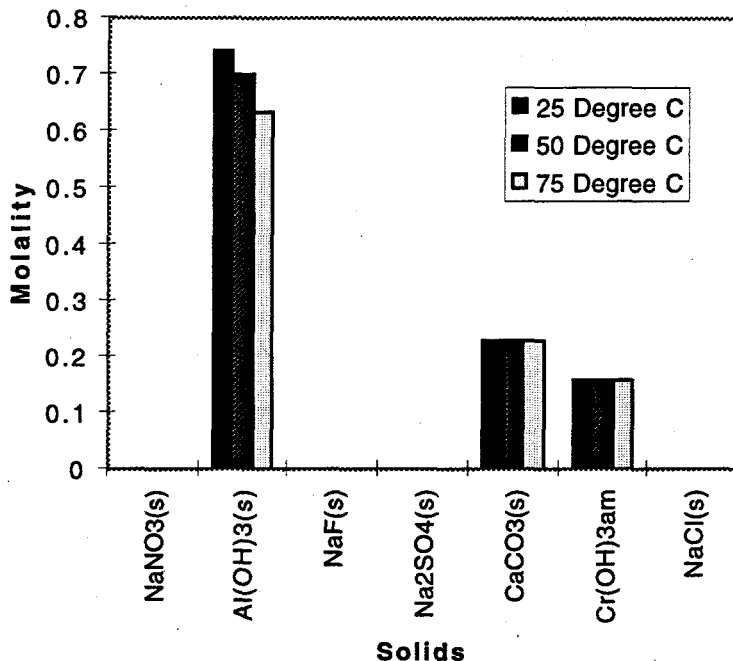


Figure 2.9. Predicted Solid Concentrations Resulting from Mixing the Tank SY-102 Sludge and Supernate at 25, 50 and 75°C

2.6 Mixture of the Sludge, Supernate, and Pure Water

We also examined the potential effects of adding pure water to Tank SY-102 as water being another diluent. We assumed that the pure water has the same volume as that of the supernate (932,000 L). Thus, this case has the volume ratio of 1:2:2 for the sludge, the supernate and the added water. The model results are reported here for 25°C.

Similar to those of the mixture of the sludge and the supernate without additional water, this case totally dissolved the Na-bearing solids, i.e., $\text{NaNO}_3(\text{s})$, thenardite, $\text{NaF}(\text{s})$, and halite at 25°C, as predicted results for the aqueous species and solids are shown in Figures 2.10 and 2.11, respectively.

These figures also show values without any chemical reactions for a comparative purpose. Even with all these four solids are dissolved they are still significantly under saturated. However, 0.0108 m of gibbsite was precipitated, reducing $\text{Al}(\text{OH})_4^-$ from 0.0313 m to 0.0205 m, while increasing OH^- to 0.2625 m by the same amount. Calcite and amorphous $\text{Cr}(\text{OH})_3$ do not change their concentrations, as before. Figures 2.12 and 2.13 show predicted chemical concentrations for the cases with and without added the added water, reflecting the effect of physical dilution of chemicals by adding water to the tank.

Solution for Sludge, Supernate & Water

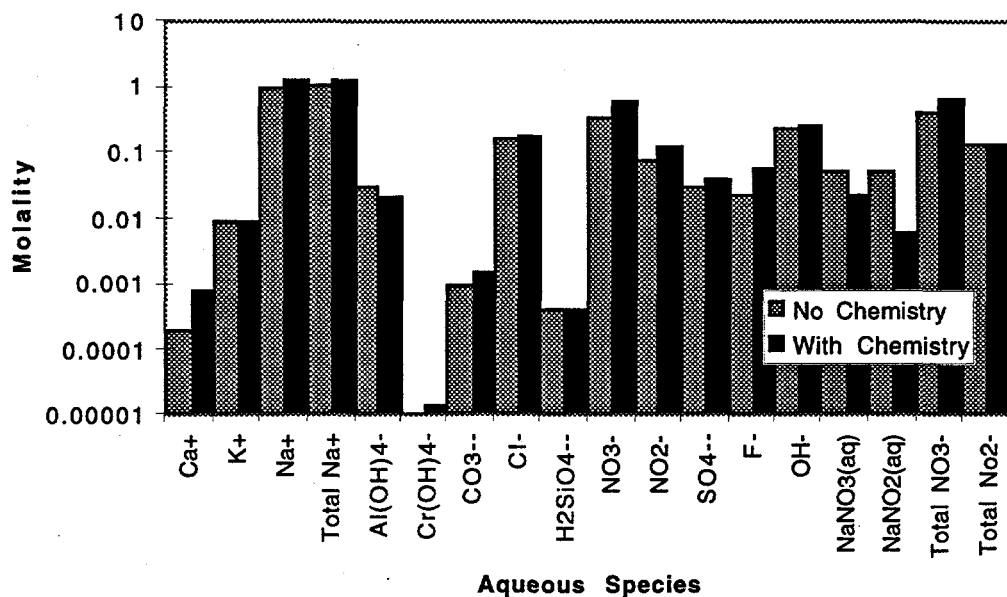


Figure 2.10. Predicted Aqueous Species Concentrations Resulting from Mixing the Tank SY-102 Sludge and Supernate with Pure Water at 25°C

Solids in Sludge, Supernate, and Water

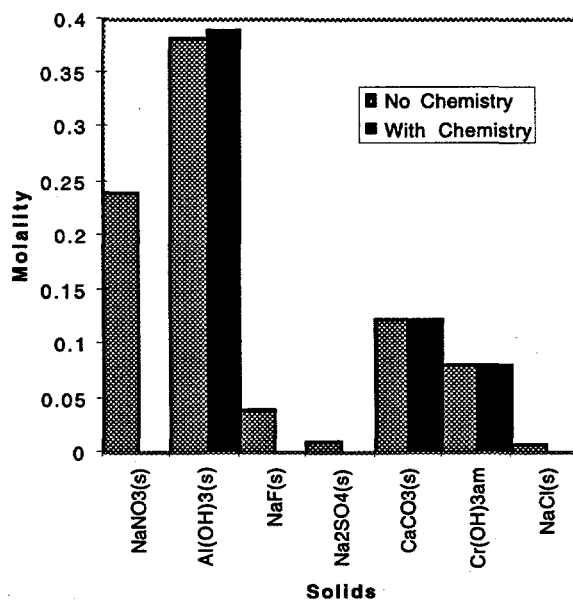


Figure 2.11. Predicted Solid Concentrations Resulting from the Tank SY-102 Sludge and Supernate with Pure Water at 25°C

With and Without Added Water

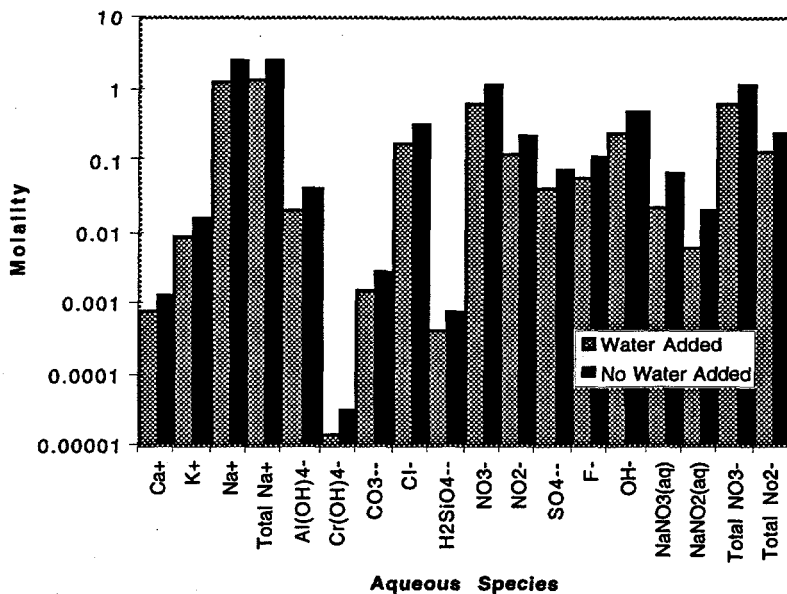


Figure 2.12. Comparison of Predicted Aqueous Species Concentrations with/Without Additional Water

Solids : With and Without Added Water

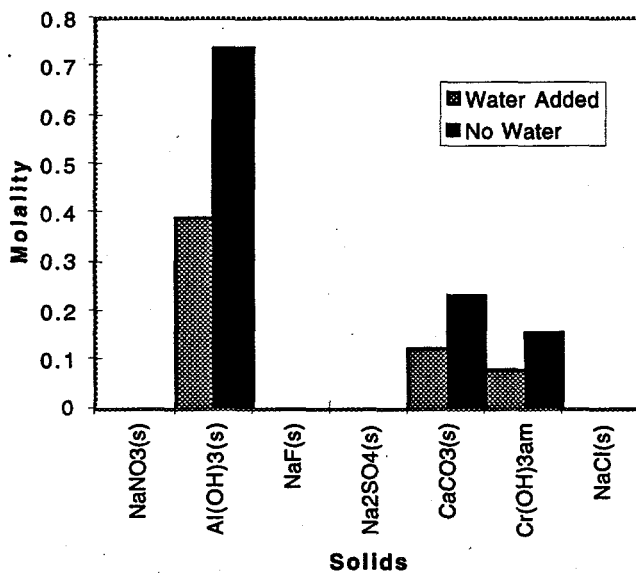


Figure 2.13. Comparison of Solids with and Without Additional Water (these results indicate that adding water does not significantly change the chemical reactions over the mixture of sludge and supernate in Tank SY-102)

2.7 Mixture of Sludge and Supernate at Temperature 25°C for Case II

Based on the interstitial solution's chemical analysis reported by DiCenso et al (1995), the current modeling indicates that only solids containing sodium are $\text{NaNO}_3(\text{s})$, thenardite, $\text{NaF}(\text{s})$, and halite. These values matched very well with the measured data on these solids. However, DiCenso et al. (1995) also reported the amount of Na which is 4.3 times more than Na contained in our $\text{NaNO}_3(\text{s})$, thenardite, $\text{NaF}(\text{s})$, and halite. Since GMIN predicted that there are no $\text{NaNO}_2(\text{s})$, $\text{Na}_2\text{CO}_3(\text{s})$, and $\text{Na}_3\text{PO}_4(\text{s})$ among the solids, we increased the amount of $\text{NaNO}_3(\text{s})$, thenardite, $\text{NaF}(\text{s})$, and halite by 4.3 times, as Case II. We did not change the amounts of non-Na-bearing solids. Following are results of Case II with increased Na^+ bearing solid molalities.

Even with these increased amounts of Na bearing solids, $\text{NaNO}_3(\text{s})$, thenardite, and halite are predicted to be dissolved out to the solution. There is a very small amount of $\text{NaF}(\text{s})$ still left as a solid, however, in this case. Consequently, Na^+ , Ca^+ , NO_3^- , F^- , SO_4^{2-} , and CO_3^{2-} were increased in the solution, as shown in Figures 2.14 and 2.15. However, a small amount (0.010 m) of gibbsite was precipitated. Changes on calcite and amorphous $\text{Cr}(\text{OH})_3$ are very small. Thus these results are similar to those discussed in Section 2.4 with much smaller Na-bearing solids in the tank.

Sludge and Supernate: Solids:2

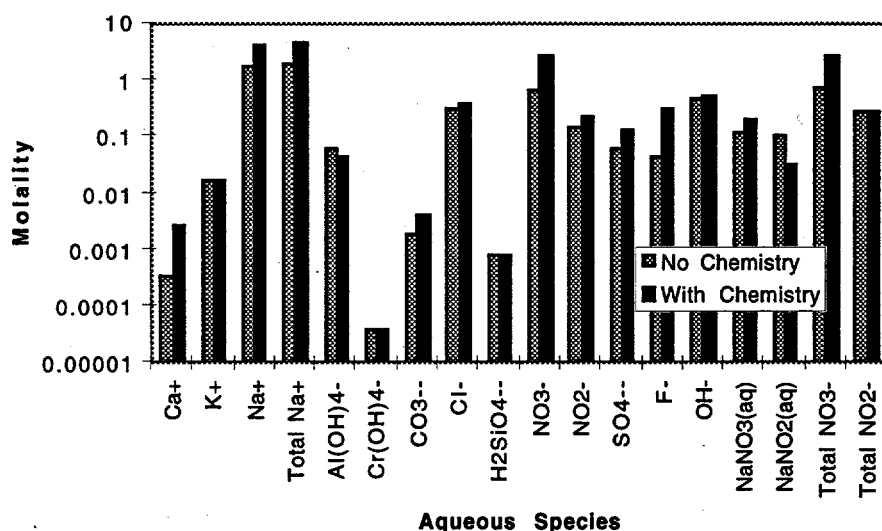


Figure 2.14. Predicted Aqueous Species Concentrations Resulting from Mixing the Tank SY-102 Sludge and Supernate at 25°C for Case II

Solids in Sludge/Supernate Mixture: 2

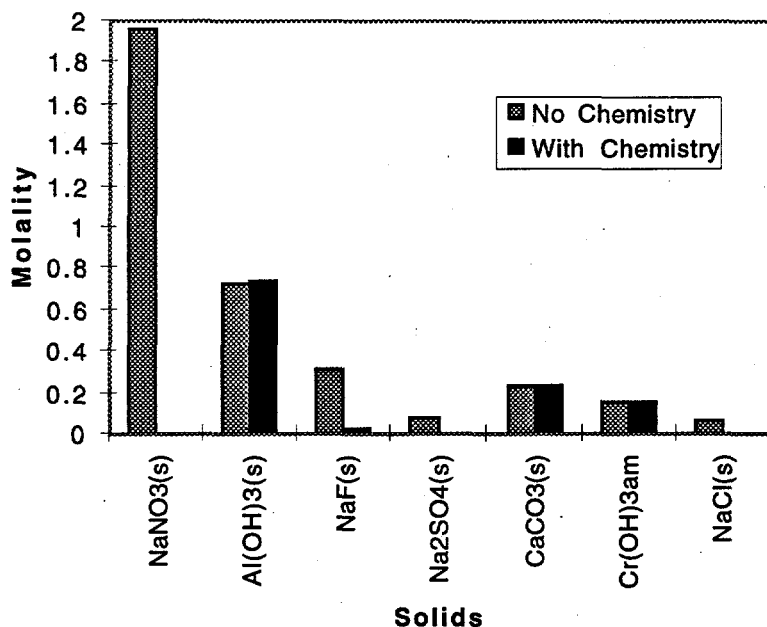


Figure 2.15. Predicted Solid concentrations Resulting from Mixing the Tank SY-102 Sludge and Supernate at 25°C for Case II

2.8 Thermal Effects on Tank Waste Chemistry for Case II

With elevated temperature of 50 and 75°C, the general trend is similar to that with the much smaller Na-containing solids case (Case I), as discussed in Section 2.5. NaNO₃(s), thenardite, and halite were all dissolved out, as at 25°C. However, NaF(s) precipitated more, as the temperature rose, (see Figure 2.16 and 2.17 showing predicted concentrations at 25, 50 and 75°C). Halite and thenardite, although they are still under saturation, are less so at these elevated temperatures than at 25°C, as in Case I.

Unlike at 25°C, due to the increase of gibbsite solubility at higher temperature, approximately 4 and 13% of the gibbsite in the Tank SY-102 are dissolved into the solution at 50 and 75°C, respectively. The corresponding concentrations of Al(OH)₄⁻ increased from 0.0422 m at 25°C to 0.087 m at 50°C and 0.157 m at 75°C. Note that predicted hydroxide concentrations were slightly lower at these higher temperatures (from 0.50 m at 25°C to 0.38 m at 75°C), possibly helping the increase of gibbsite solubility. As shown in Figures 2.16 and 2.18, changes of calcite and amorphous Cr(OH)₃ at 50, and 75°C are minimum.

Solution with More Solids: 2

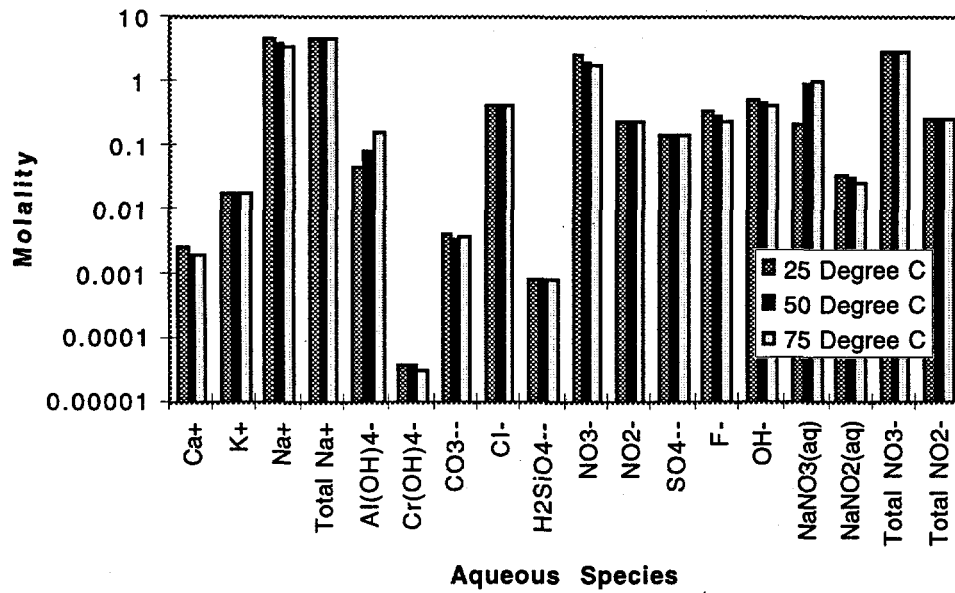


Figure 2.16. Predicted Aqueous Species Concentrations Resulting from Mixing the Tank SY-102 Sludge and Supernate at 25, 50 and 75°C for Case II

More Solids in Sludge: 2

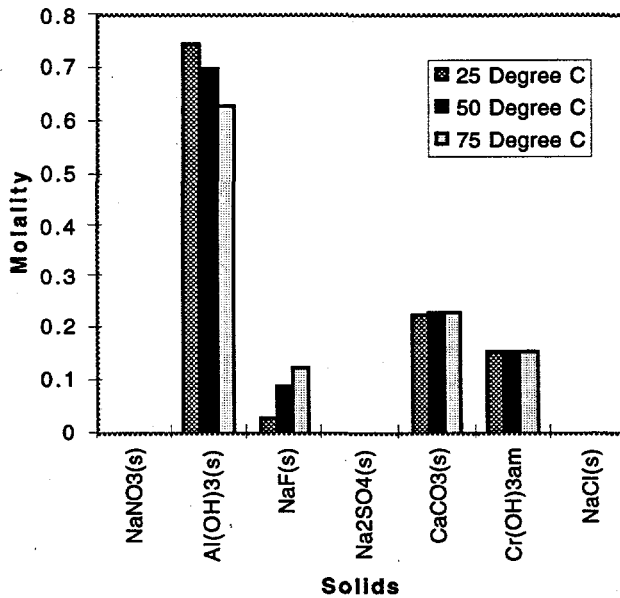


Figure 2.17. Predicted Solid concentrations Resulting from Mixing the Tank SY-102 Sludge and Supernate at 25, 50 and 75°C for Case II

Solution for Sludge/Supernate/Water: 2

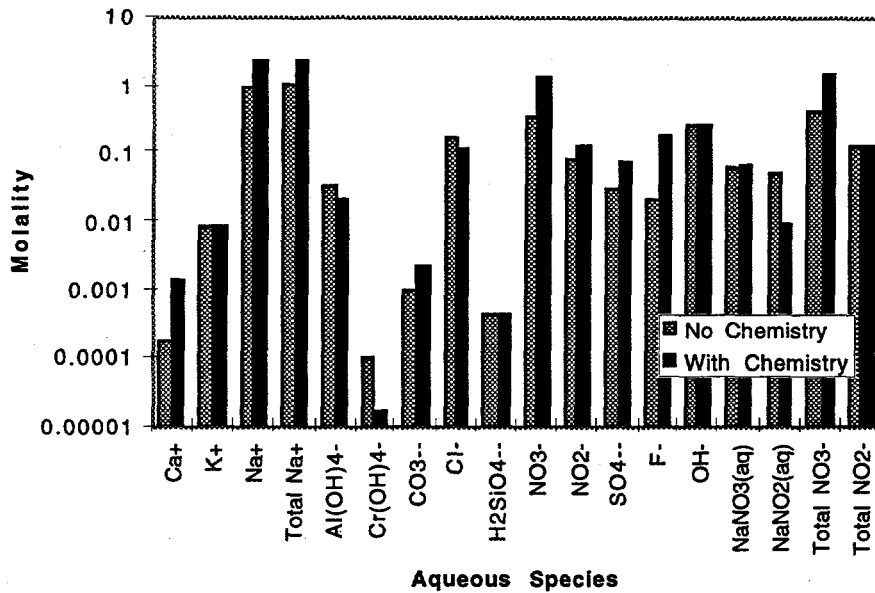


Figure 2.18. Predicted Aqueous Species Concentrations from the Mixture of Tank SY-102 Sludge and Supernate with Pure Water at 25°C for Case II

These model results are very similar to the cases without increasing N-containing solids, as discussed above, thus reducing uncertainty by the amount of Na-bearing solid amounts. The modeling study suggests that at higher temperature, most of the Na-bearing solids are dissolved. Also gibbsite will not precipitate, but dissolved, thus reducing potential problems associated with gibbsite precipitation. Calcite and amorphous $\text{Cr}(\text{OH})_3$ are not significantly affected.

2.9 Mixture of the Sludge, Supernate, and Pure Water for Case II

We also examined the potential effects of adding pure water to Tank SY-102 as before, this time including 4.3 times more Na-containing solids. We assumed that pure water has the same volume as that of the supernate (932,000 L). Thus, this case also has the volume ratio of 1 : 2 : 2 for the sludge, the supernate, and the added water. The model results reported here are at 25°C.

Similar to those of the mixture of the sludge and the supernate without additional water, this case totally dissolved all Na-containing solids, $\text{NaNO}_3(\text{s})$, thenardite, $\text{NaF}(\text{s})$, and halite at 25°C, as predicted results for the aqueous species and solids are shown in Figures 2.18 and 2.19, respectively.

Solids for Added Water: 2

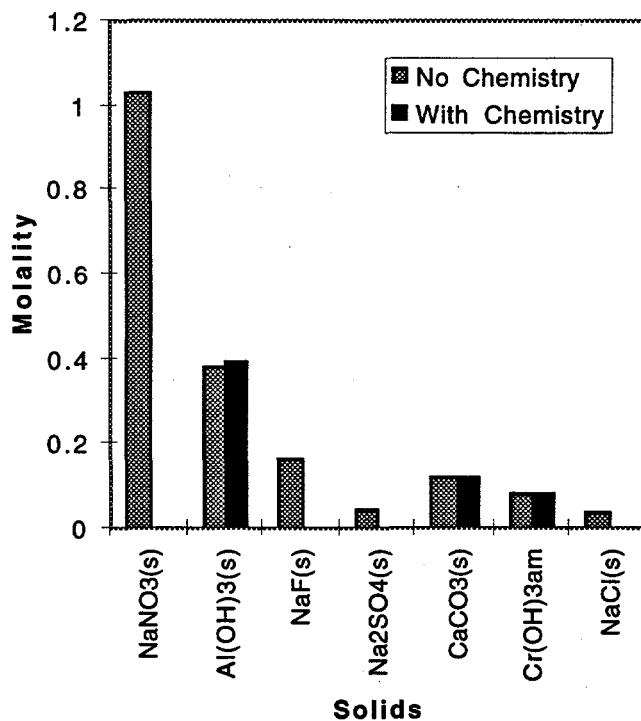


Figure 2.19. Predicted Solid Concentrations Resulting from the Mixture of Tank SY-102 Sludge and Supernate with Pure Water at 25°C for Case II

These figures also show values without any chemical reactions for a comparative purpose. These results are similar to Case I (with much smaller amounts of Na-bearing solids) discussed in Section 2.6. However, 0.0108 m of gibbsite was precipitated, reducing Al(OH)_4^- from 0.0313 m to 0.0209 m, while increasing OH^- to 0.262 by the same amount. Calcite and amorphous Cr(OH)_3 remain unaffected.

These model results indicate that adding water does not significantly change the chemical reactions of the mixture of sludge and supernate already in Tank SY-102.

3.0 Transport Behavior

Because transport of the retrieved slurry will use the new Cross-Site Transfer System (CSTS), the waste acceptance criteria for this system will apply. The CSTS is currently in the final design and procurement phase of construction during this documentation. Because of this, the current functional design criteria (WHC 1995) will function as the reference waste acceptance criteria in this assessment. However, the criteria applicable at the time of the transport may differ from this somewhat once as-built systems specifications become available. For this reason, in this section we estimate the pressure drops that will be required to deliver the resulting slurries and compare them with the current functional design criteria. These estimates are intended to broaden the application of the available data to the extent that an acceptance decision can be easily made.

3.1 CSTS Transport Criteria

The functional design criteria document (WHC 1995) indicates that the CSTS will be capable of transporting slurries with the specifications summarized in Table 3.1.

Of the five criteria, only the solids content requires clarification. What is usually intended by "solids content" or "displaced solids volume" is a settled slurry fraction that results from a short time settling of the slurry. In practice, this is typically measured by allowing stagnant slurry in a vertical tube to settle for several minutes. The height of the settled slurry which results is divided by the total height of the tube to obtain the fractional solids content. Thus, the solids content referred to in these specifications includes the whatever volume is occupied by interstitial liquid as well. To predict the relationship between this value and the volume actually occupied by the solid phase requires an understanding of the colloidal nature and chemistry of the slurry system.

For this reason, in this document we will give a limited discussion on the settled slurry fraction, documenting some applicable sedimentation experiments which were performed with the waste material. We will focus instead on the volume of the solid phase (hereafter referred to as the solids volume fraction) which plays an important role in the prediction of the energy (or pressure drop) required to transport the slurry while sustaining particle suspension.

Certain solid phase waste species which are commonly present in the Hanford tank waste can present behavior which are not typically modeled in slurry transport correlations which are used for engineering design and analysis. For example, the presence of certain colloidal particulate can result in significant deviations from Newtonian rheology. Also, some salts common to these waste streams can form high aspect ratio crystals the effects of which are typically not accounted for in the engineering models. Some of the solid phase species which are known to give problems of this type include species containing aluminum or iron and phosphate salts.

Table 3.1. Slurry Acceptance Criteria Based on the CSTS Function Design Criteria (WHC 1995)

Criteria	Specification
Specific Gravity	1.0 to 1.5
Viscosity	1.0 to 30 cP
Solids Content	0 to 30%
pH Range	11.0 to 14.0
Temperature	80 to 200°F

3.2 Specie Specific Rheological Behavior

3.2.1 Aluminum

As mentioned in Section 2, several aluminum species, including sodium aluminate, amorphous aluminum hydroxide, gibbsite, and boehmite, have been observed in Hanford tank wastes. According to the phase map of Barney (1976) and the arguments presented in Section 2, we expect that the predominate solid phase aluminum specie in Tank 241-SY-102 is gibbsite (see Figure 2.1 and the related discussion in Section 2.) Transmission electron microscopy (TEM) analyses are being performed on waste samples from the 1990 SY-102 core sampling event. The results of these tests should determine what phases are actually present in the waste. In this section, we briefly describe the expected contributions of each aluminum hydroxide phase which is potentially present.

Amorphous Aluminum Hydroxide

Amorphous aluminum hydroxide is perhaps the least desirable solid aluminum phase because it presents the most problems in waste transport. As the concentration of this amorphous phase reaches the gel point, the effective viscosity of the waste solution increases dramatically resulting in pressure drop requirements for transport which are not practically obtainable. The amorphous phase is thought to precipitate from dissolved aluminum at low sodium hydroxide concentrations when its concentration rises or when temperature or concentration changes reduce the solubility limit. This amorphous phase is thought to be converted to the gibbsite phase after relatively short times (i.e., hours to days). The key to avoiding the amorphous aluminum hydroxide gel is to *disallow precipitation of aluminum hydroxides* during mobilization and retrieval. (The effects of potential gel formation are *not* included not included in the engineering calculations which predict the energy required for slurry transport.)

Gibbsite

From a transport perspective, gibbsite is the most desirable of the common solid phase aluminum hydroxide species and is most likely the predominant solid aluminum phase in the 102-SY waste. Gibbsite typically forms roughly spherical shaped primary particles which are colloidal in size (i.e., less than 1 μm) and nature; these particles have been observed in waste streams as stable agglomerates which are typically between 10 and 100 μm . [This size range is consistent with the particle size distribution for 102-SY reported by DiCenso et al. (1995).]

The presence of gibbsite in the waste can result in slurry rheologies which deviate noticeably from Newtonian behavior. Bunker et al. (1995a) report measurements of up to 4.2 vol% gibbsite in 1 M NaOH solutions that exhibit a noticeable shear-thinning behavior. At shear rates of approximately 100 s^{-1} , the apparent viscosities were somewhat below 20 cP. (As will be discussed below, this viscosity regime is consistent with the rheology data for SY-102 reported in DiCenso et al. [1995].)

The authors believe that gibbsite *may* be adequately modeled in the engineering transport models due to the relatively large agglomerate size and small aspect ratio (i.e., nearly spherical shaped) particles which have been observed in the wastes. However, there is almost a complete dearth of information regarding the effects of gibbsite under typical transport conditions. Therefore, adequate conservatism should be included in the appropriate transport criteria when gibbsite is thought to be present to reduce the risk of problems during the cross-site transfer.

Boehmite

Boehmite forms extremely small (i.e., 10 to 50 nm) primary particles with agglomerates typically in the near-colloidal size (i.e., around 1 μm) regime. Even at relatively low concentrations, the presence of boehmite in waste slurries can result in significant deviations from Newtonian rheology. Bunker et al. (1995b) have performed series of rheology

experiments with boehmite suspensions. These have demonstrated dramatic shear-thinning behavior. For example, their results indicate that a 1 vol. % boehmite suspension (in 1 M NaNO₃ and 1 M NaOH) has an apparent viscosity of over 400 cP at 10 s⁻¹, while at 100 s⁻¹ the apparent viscosity is about 50 cP.

Thus, the presence of boehmite in the waste slurries can result in dramatic effects which are not accounted for in the engineering calculations which predict the required energy for slurry transport. Fortunately, boehmite is not thought to occur in significant quantities in Tank 241-SY-102.

3.2.2 Iron Hydroxides

The presence of iron hydroxides in the waste slurry can present similar challenges to waste transport as those observed with the boehmite aluminum phase. Bunker et al. (1995b) report a series of rheology measurements with iron hydroxide suspensions, some of which were performed with high ionic strength solutions. For a 3.25 vol% Fe(OH)₃ suspension near pH 12 (at low salt concentrations), they observed apparent viscosities of approximately 1300 cP at shear rates of about 10 s⁻¹. For the same suspension, an apparent viscosity of approximately 200 cP was observed at a shear rate of 100 s⁻¹.

Based on this information, it is *unlikely* that the effects of significant concentrations of iron hydroxides are effectively modeled by the current engineering calculations which predict the energy required for slurry transport.

3.2.3 Phosphates

The presence of phosphate salts in the solid phase of the waste can also present challenges to waste transport. In fact, precipitation of phosphate salts during transport may have resulted in the plugging of several of the existing cross-site transfer lines. However, (as discussed in Section 2) the concentration of phosphates in the SY-102 waste is predicted to remain well below the solubility limit; therefore, appreciable phosphate solids are not anticipated in the current mobilization and retrieval scenarios. A more extensive review on the potential hazards related to the transport of phosphates is given by McKay.^(a)

3.3 Settled Slurry Volume Fraction and Sedimentation Behavior

As mentioned earlier, the design criteria for the CSTS (WHC 1995) indicates that this system will be capable of transferring waste with solids contents of up to 30%. From the way this is typically obtained, the solids content is a measure of the short-time sedimentation behavior of the waste. As stated earlier, this behavior is difficult to predict without detailed knowledge of the colloidal nature of the solid species. However, we can provide some information about this behavior from sedimentation experiments performed with the 102-SY waste samples from the 1988 core sampling event and from similar experiments in the literature.

DiCenso et al. (1995) report sedimentation experiments in which material taken from Segment 4B (that nearest the tank bottom) of the 1988 sampling event was diluted with deionized water and allowed to settle. Two dilutions were performed, one at 1:1 (deionized water:waste) and the other at 2:1. Neither of these samples settled significantly within the first few minutes. After one hour, the 1:1 diluted sample had still not settled, while the 2:1 diluted sample had settled 0.4 cm (about 7% of the 6.13 cm total height). Therefore, the field measurement for this quantity would likely indicate a solids content near 100% for both of these solutions.

(a) McKay, R. L. 1993. *TWRS Retrieval Technology Project: Slurry Transport Plugging Investigation*. Letter Report, Pacific Northwest National Laboratory, Richland, Washington.

At longer times each of the diluted samples settled significantly. For the 1:1 diluted sample, asymptotic behavior was reached after about three days with the total amount settled at about 2.8 cm (42% of the total height of 6.67 cm). For the 2:1 diluted sample, the solids settled 3.8 cm (62% of the 6.13 cm total height) in about 24 hours. This behavior is consistent with that commonly observed in the sedimentation of certain metal hydroxides (see, for example Glasrud et al. 1993) and has been observed with both Hanford wastes and waste simulants (Rector and Bunker 1995).

Unfortunately, since the dilutions were performed with deionized water (instead of tank supernatant liquid or an equimolar sodium hydroxide and salt solution), differences in waste chemistry make applying these results to the current mobilization and retrieval scenario rather difficult. However, it seems apparent that this criteria, if enforced as a waste acceptance criteria, will be difficult to attain at small dilution ratios.

Finally, there is no simple relationship between the settled slurry volume fraction and energy requirements for slurry transport. A well dispersed suspension of metal hydroxides can result in large settled slurry fractions which are easily transported while large salt crystals (which settle easily) can result in very low settled slurry fractions that require very high transport energies. Because of this, settled slurry fraction is not a useful criteria for waste acceptance in a transport system.

3.4 Waste Property and Transport Behavior Estimates

In this section, we use the estimates of chemical and phase composition presented in Section 2 to predict the expected transport behavior of the slurries which will result from mixing the current Tank 241-SY-102 contents and from a potential water addition. Following the precedent in Section 2, the cases considered here are those summarized in Table 3.2. Estimates of waste properties related to the functional design criteria and estimates of slurry transport behavior are made in this section for several temperatures (25, 50, 75 and 100°C) for the supernatant liquid and slurry mixtures. Estimates of the water addition cases were performed only at 25°C.

3.4.1. Rheology of the Waste Mixtures

Determination of both the pure liquid and mixture viscosities are an extremely important part of estimating the energy requirements for slurry transport. As will be discussed more fully below, the rate at which particles settle in the slurry is a function of (among other variables) the pure liquid viscosity. Because of this the transport velocity required to maintain particle suspension is sensitive to changes in the liquid viscosity. The energy (or pressure drop) required to maintain the transport velocity is a function of the mixture viscosity.

Table 3.2. Summary of Slurry Transport Cases

Case	Descriptor	Sludge Compositions
Supernatant liquid and slurry mixture (SSM)	I-A	Na salts as reported by DiCenso et al. (1995)
SSM with water addition	I-B	Na salts as reported by DiCenso et al. (1995)
SSM	II-A	Increased Na salts as required by Na balance
SSM with water addition	II-B	Increased Na salts as required by Na balance

General Theory and Available Correlations

The liquid viscosities were estimated using the model suggested by Mahoney and Trent (1995),

$$\mu_L = a_4 \exp([a_0 + a_1\chi + a_2\chi^2]/T) \quad (3.1)$$

where a_k are the coefficients fit from experimental data, T is the solution temperature and χ is the weight percentage of the solute. Mahoney and Trent tabulate values for these constants based on the viscosity data obtained from the literature for NaNO_3 solutions. The correlation is thought to give estimates that are within 10 % of the actual value for solutions with 0 to 90 wt% NaNO_3 in the temperature range from 273 to 433 K. The coefficients values are given in Table 3.3. While the SY-102 liquid is much more complex than a simple NaNO_3 solution, this model should give a meaningful variation of the liquid viscosity with changes in the dissolved solids. For the current analysis, we will use the total dissolved mass percentage for χ . Because of this, the expected uncertainty in this measurement is likely to be larger than the 10% value given earlier. However, as will be shown later, the analysis is not sensitive to small errors (e.g., 30%) in the liquid viscosity.

No comprehensive mixture viscosity correlation is available for the wastes due to the complexity of the solid-liquid mixtures and their interactions. The development of such a relationship for uniform spherical particles has been the subject of numerous theoretical and experimental efforts. One common approach is to extend Einstein's viscosity relationship to apply at finite particle volume concentrations. The type of relationship which results is typically of the form

$$\mu_M = \mu_L(1 + 2.5C_V + 14.4C_V^2 + \dots) \quad (3.2)$$

where C_V is the particle volume fraction and the ellipse indicates higher order terms. Similar expressions have been given by a number of authors (see, for example, Frankel and Acrivos, 1967). Relationships of this form apply for uniform spherical particles with low to moderate particle volume loadings. As the particulate volume loading approaches maximum packing, the predicted viscosities will deviate significantly from those observed.

Equation 3.2 is used in this effort to relate the effect of particle volume loading on the waste mixture viscosity. While the solids in the waste mixture are far from uniform spheres, this equation is a vehicle for introducing the solids volume fraction effect. A model of this form *does not include* any colloidal or large aspect ratio effects. Because of the colloidal effects (particularly with the aluminum and iron phases) mentioned in Section 2, the effect of solids loading on the mixture viscosity may be much more non-linear than that predicted by Equation 3.2.

Table 3.3. Coefficients for Equation 3.1 (based on experimental measurements of NaNO_3 solutions taken from Mahoney and Trent 1995)

a4	5.8044 x 10 ⁻⁶ Pa-s
a1	1489.9
a2	-0.97874
a3	0.19490

Experimental Evidence

According to DiCenso et al. (1995), a number of physical measurements related to the sludge from Tank 241-SY-102 are available from the 1988 core sampling event. These include data suggesting the effect of dilution on the rheology of resulting waste slurries. Apparent viscosities were evidently measured as a function of both shear rate and dilution for dilution ratios of 1:1 (deionized water: segment 4B [bottom layer] solids composite) and 2:1 at 30 °C and fit to a power law equation of the form

$$\mu_M = \beta \dot{\gamma}^{(n-1)}, \quad (3.3)$$

where $\dot{\gamma}$ is the shear rate, β is the consistency factor and n is the behavior index. The data from the 2:1 dilution indicate that the mixture was shear-thinning ($n = 0.8$), with a consistency factor of approximately 0.014 Pa-s (14 cP). If this slurry is transported in a three inch pipe at 3 ft/s, the average shear rate experienced is

$$\frac{U_b}{r} = \frac{36 \text{ in/s}}{3 \text{ in}/2} = 24 \text{ s}^{-1}. \quad (3.4)$$

Therefore, we might expect average shear rates during transport in the cross-site line to be on the order of 10 s^{-1} . Using Equation 3.3, this shear rate corresponds to a viscosity of 0.0088 Pa-s (8.8 cP), roughly ten times the viscosity of water at 20°C.

Current Approach

While we expect the waste mixture to experience a large variety of shear rates due to turbulence, using an average shear rate (and the viscosity associated with that shear rate) will result in conservatively high values for the mixture viscosity and the associate required energy for waste transport. This approach is conservative because most of the energy losses due to transport occur within the flow region very near the wall of the pipe. In this region the shear rates are much larger than the average; therefore, the apparent viscosities in this region are much lower than those predicted by our approach.

In the absence of experimental data which indicate the rheology of these mixtures under transport conditions, we will use a relationship of the same form as Equation 3.2 to include the effect of solids loading. However, since the experimental measurement (as described by DiCenso et al. [1995]) indicate that larger viscosities have been observed, the predicted viscosities are increased by a factor of ten (corresponding to the factor of ten increase over water discussed above). Therefore, the relationship for mixture viscosity used in this effort is

$$\mu_M = 10 \mu_L (1 + 2.5C_v + 14.4C_v^2) \quad (3.5)$$

3.4.2 Predictions of the Energy Required for Waste Transport

The pressure drop required for transport is a measure of how much energy is required to maintain particle suspension during the waste transfer. A number of waste property estimates and intermediate quantities are required to calculate this pressure drop. The estimate or calculation method for each of these quantities is described below.

Liquid Density

The density of the Tank SY-102 solution was calculated by using an empirical formula for a multi-component solution developed for tank wastes (Mahoney and Trent 1995). Based on this formula, the solution density, ρ_c (kg/m^3) is computed by

$$\rho_c = 1245.8 - 9.824C - 1.0606T + 0.6812T^2 \quad (3.6)$$

where C is the weight percent of the all aqueous species to the total solution weight. Based on the molality of each aqueous species in the solution and its molecular weight, we calculated the weight percentage of the total aqueous species to the solution weight. However, this formula yields the solution density of the sludge and supernate to be 1,038 and 1,372 kg/m^3 , whereas, DiCenso et al (1995) reported these values to be 1,030 and 1,180 kg/m^3 . Thus the density values calculated by Equation 3.6 were further adjusted by the following linear function to compensate the error produced by the empirical formula, Equation 3.7:

$$\rho_a = 0.4491\rho_c + 563.8 \quad (3.7)$$

where ρ_a is the actual solution density (kg/m^3) used in this study.

Liquid Viscosity

Liquid viscosity is calculated using Equation 3.1 with the coefficients from Table 3.2. The total mass percentage of solids in the solution is used in the place of the NaNO_3 mass percentage.

Solid Density

A value of 1800 Kg/m^3 (that given by DiCenso et al. [1995] for solids density) is assumed throughout the calculation regardless of what solids are present. The impact of this assumption is discussed below.

Solid Weight Fraction

Solid weight fraction is taken from a mass balance during the chemical and phase equilibrium calculations. Since iron, lead and manganese are not included in these calculations, they are assumed to be "insoluble" and remain in the solid phase. According to the analyte concentrations given by DiCenso et al., the sludge solids contains approximately 4.7 wt. % $\text{Fe}(\text{OH})_3$ (assuming this is the only iron species). Lead and manganese hydroxides account for less than 2 wt. % of the sludge solids. Therefore it is assumed in these calculations that 7 wt. % of the sludge solids are iron, lead and manganese hydroxides (as well as any other insoluble species).

These "insoluble" solids are taken to be at the same density as the other sludge material so that they also consist of 7 vol% (17.3 m^3) of the sludge solids. Thus, this insoluble phase is 4.2 vol% of the slurry in the current waste configuration, 1.4 vol% of the waste slurry in the mixed condition, and 0.8 vol% of the mixed slurry after the water addition (discussed below).

Mixture Density

Mixture density is a function of the solid and the liquid density as well as the solids fraction. Another measure of mixture density is the specific gravity, which appears in the functional design criteria. Mixture density is calculated from a definition of the solids mass fraction,

$$\chi_s = C_v \frac{\rho_s}{\rho_M} \quad (3.8)$$

and a phase mass balance,

$$\rho_M = \rho_s C_v + \rho_L (1 - C_v) \quad (3.9)$$

Equations 3.8 and 3.9 can be rearranged, eliminating C_v , giving

$$\rho_M = \frac{\rho_L}{\left(1 - \chi_s \left(1 - \frac{\rho_L}{\rho_s}\right)\right)} \quad (3.10)$$

Mixture Viscosity

Estimated (as discussed above) using Equation 3.5.

Specific Gravity

Estimated by dividing the mixture density (in Kg/m³) by 1000.

Particle Settling Velocity

This is the velocity at which a particle settles in a stagnant fluid (without the influence of other particles). For small particles in liquid (i.e., for Stokes flow), this may be calculated as

$$V_s = \frac{g(\rho_s - \rho_L)d^2}{18 \mu_L} \quad (3.11)$$

where g is gravitational acceleration and d is the particle diameter.

Particle Drag Coefficient

The particle drag coefficient is a measure of how well the particle responds to fluid motions. In most Hanford waste applications this can be calculated as

$$C_D = \frac{24 \mu_L}{dV_s \rho_s} \quad (3.12)$$

Critical Velocity

The critical velocity for slurry transport is that below which particulate suspension is no longer maintained. The lowest energy requirements (i.e., the lowest pressure drops) are associated with transporting the slurry at this bulk velocity. Correlations for the critical velocity are given by a number of authors. For this effort, we use the correlation of Zandi and Govatos (1967) because of the following attractive features:

- a large number of data were included in the study (approximately 1500 data points)

- it includes the effects of changes in the carrier liquid viscosity and solids loadings
- the terms in this correlation are analytical (no additional nomographs are needed)
- it gives values which are conservative relative to (higher than) those of other correlations which have similar features.

The Zandi and Govatos correlation gives the critical velocity as

$$V_{M2} = \sqrt{\frac{40 C_v D g \left(\frac{\rho_s}{\rho_L} - 1 \right)}{\sqrt{C_D}}} \quad (3.13)$$

where D is the pipe diameter. The correlation of Zandi and Govatos (1967) gives similar results to that of Durand (1953) when the viscosity of the carrier fluid is that of water.

Operating Velocity

In industry, the operating velocity, V_o , is typically chosen to be 20 to 40% in excess of the critical velocity to ensure that particulate suspension is maintained. For the current analysis, we use an operating velocity which is 60% greater than the critical velocity to provide a sufficient safety margin for the CSTS.

Bulk Reynolds Number

The bulk Reynolds number, Re_b , provides a description of the flow regime which is expected for Newtonian slurries. For Reynolds numbers in excess of 10,000, the flow is fully turbulent. For Reynolds numbers below 2000, the flow is expected to be laminar. For $2,300 < Re_b < 10,000$, the flow may be described as being in transition to turbulence, or as in "low Reynolds number" turbulence. Fully developed flows are not *always* required to maintain particulate suspension.

The Reynolds number is defined as

$$Re_b = \frac{U_b D \rho_M}{\mu_M} \quad (3.14)$$

where U_b is the bulk (or average) velocity. For these calculations, we use the operating velocity as the bulk velocity for the Reynolds number calculations.

Required Flowrate

The required flowrate, Q , is that necessary to achieve the operating velocity. This is calculated as

$$Q = 2\pi \frac{D^2}{4} V_o \quad (3.15)$$

Darcy (Mixture) Friction Factor

The Darcy friction factor is required for the pressure drop estimate. It is calculated assuming a smooth pipe by

$$f_{D,M} = 4 (0.0791) \text{Re}_b^{-0.25} \quad (3.16)$$

This friction factor includes the effects of the solids in the mixture because the Reynolds number is calculated using the mixture density and viscosity.

Required Pressure Drop

The pressure drop is estimated by

$$\Delta P = f_{D,M} \frac{L_E}{gD} \frac{V_o^2}{2} \quad (3.17)$$

where L_E is the total equivalent length of the transfer line.

3.4.3 Slurry Transport Evaluations

The relationships developed in the previous section were applied for each case considered in Section 2 and estimates of the energy required to maintain particulate suspension were obtained as pressure drops for each case. A summary of information related to these estimates is given for Cases I and II in Tables 3.4 and 3.5.

The following additional *assumptions* were made as a part of these estimates:

- The pipe diameter was taken to be that of Schedule 40, 3-in., seamless pipe (3.068 in.).
- The total equivalent pipe length was taken to be 38,000 ft (7.2 miles or 11,600 m).
- The particle size was taken to be 120 μm . This is near the upper end of the SY-102 particle size distribution reported by DiCenso et al. (1995).
- Any changes in head due to differences in elevation are not considered.

The following *caveats* apply to these estimates:

- As discussed earlier, the viscosity estimates which are made from assuming uniform spherical particles are clearly not consistent with the rheology information presented by DiCenso et al. (1995). The viscosity estimates made here were obtained using Equation 3.5. However, while this relationship may give conservative (higher than actual) values for the energy required for waste transport, it is not considered rigorous. Indeed, where significant volume fractions of metal hydroxides are present, the nonlinearity of the solid volume effect may be under-predicted by Equation 3.5.
- As noted earlier, the critical velocity correlation of Zandi and Govatos (1967) gives estimates based on a large number of experimental data. However, very few of these data include the complexity of slurry that is expected from Hanford waste (due to large variations in particulate size, colloidal and chemical constituency). In the absence of data which could be used to suggest a more rigorous approach, an operating velocity which includes a 60% increase over the critical velocity is used to build conservatism into the estimate and account for this uncertainty.

Table 3.4. Summary of Estimates for Case I (case descriptor "A" indicates a case in which the current tank contents [sludge and supernatant liquid] are mixed; descriptor "B" indicates a case in which additional water is added according to the discussion in Section 2)

Case descriptor			A	A	A	A	B
T	°C		25	50	75	100	25
Liquid							
Density	Kg/m ³		1076	1070	1065	1065	1022
Viscosity	Pa-s		0.0010	0.0006	0.0005	0.0003	0.0009
	cP		1.0	0.6	0.5	0.3	0.9
Solid							
Density	Kg/m ³		1800	1800	1800	1800	1800
Weight fraction	w/o "insolubles"		0.061	0.059	0.055	0.051	0.039
	"insolubles"		0.019	0.019	0.019	0.019	0.012
	Total		0.080	0.078	0.074	0.070	0.051
Volume fraction			0.049	0.048	0.045	0.043	0.030
Mixture							
Density	Kg/m ³		1112	1105	1098	1096	1045
Viscosity	Pa-s		0.0111	0.0075	0.0053	0.0039	0.0095
	cP		11.1	7.5	5.3	3.9	9.5
Specific gravity			1.11	1.10	1.10	1.10	1.04
Transport Behavior							
Settling velocity	m/s		0.0060	0.0089	0.0125	0.0166	0.0069
	ft/min		1.17	1.75	2.46	3.27	1.37
Particle drag coefficient			17.7	8.0	4.1	2.3	14.1
Critical velocity	m/s		0.49	0.59	0.69	0.77	0.43
	ft/s		1.61	1.94	2.25	2.52	1.40
Operating Velocity (+ 60 %)	m/s		0.78	0.95	1.10	1.23	0.68
	ft/s		2.57	3.11	3.61	4.03	2.25
Bulk Reynolds number			6,170	11,000	17,820	26,730	5,840
Required flowrate	m ³ /s		0.0037	0.0045	0.0052	0.0059	0.0033
	gal/min		59	72	83	93	52
Darcy friction factor			0.0357	0.0309	0.0274	0.0247	0.0362
Required pressure drop	KPa		1860	2330	2760	3120	1350
	psi		270	338	401	452	196

Table 3.5. Summary of Estimates for Case II (case descriptor "A" indicates a case in which the current tank contents [sludge and supernatant liquid] are mixed; case descriptor "B" indicates a case in which additional water is added according to the discussion in Section 2)

Case descriptor			A	A	A	A	B
T	°C		25	50	75	100	25
Liquid							
Density	Kg/m ³		1117	1110	1104	1104	1029
Viscosity	Pa-s		0.0012	0.0008	0.0006	0.0004	0.0009
	cP		1.2	0.8	0.6	0.4	0.9
Solid							
Density	Kg/m ³		1800	1800	1800	1800	1800
Weight fraction	w/o "insolubles"		0.061	0.061	0.058	0.055	0.039
	"insolubles"		0.019	0.019	0.019	0.019	0.012
	Total		0.080	0.080	0.077	0.074	0.051
Volume fraction			0.051	0.051	0.049	0.046	0.030
Mixture							
Density	Kg/m ³		1152	1145	1138	1136	1052
Viscosity	Pa-s		0.0140	0.0092	0.0062	0.0048	0.0102
	cP		14.0	9.2	6.2	4.8	10.2
Specific gravity			1.15	1.14	1.14	1.14	1.05
Transport Behavior							
Settling velocity	m/s		0.0046	0.0069	0.0099	0.0133	0.0064
	ft/min		0.90	1.36	1.94	2.62	1.26
Particle drag coefficient			28.7	12.5	6.2	3.4	16.3
Critical velocity	m/s		0.42	0.52	0.61	0.69	0.41
	ft/s		1.39	1.71	2.02	2.28	1.34
Operating velocity (+60 %)	m/s		0.68	0.83	0.98	1.11	0.66
	ft/s		2.2	2.7	3.2	3.7	2.2
Bulk Reynolds number			4,430	8,180	13,600	20,900	5,250
Required flowrate	m ³ /s		0.0032	0.0040	0.0047	0.0053	0.0031
	gal/min		51	63	74	84	50
Darcy friction factor			0.0388	0.0333	0.0293	0.0263	0.0372
Required pressure drop	KPa		1560	2020	2450	2810	1280
	psi		226	293	355	408	186

3.4.4 Results of the Transport Behavior Predictions

Several trends are worth noting from behavior predictions summarized in Tables 3.4 and 3.5. These include the following:

- The mixture viscosity decreases with increasing temperature largely because of the related decrease in liquid viscosity (the solids loading also decreases somewhat with increases in temperature). This results in higher particle settling rates and, therefore, higher critical velocities and higher pressure drop requirements for transport.
- The pressure drops predicted for Case II are somewhat lower than those predicted for Case I. This may initially seem counter-intuitive as more solids are being transported in Case II. However, the particle settling velocity is a sensitive function of the liquid viscosity and the small differences between the two cases (with Case I having the lower viscosity) result in Case I having the larger critical velocities and, therefore, the larger associated pressure drops.
- The addition of water does have the desired effect of lowering the solids fraction to be transported and lower predicted pressure drops occur for these cases. Unfortunately, using Equation 3.5 to estimate the viscosity for the waster addition cases is probably a poor choice as it is unduly pessimistic. However, no data are available to suggest alternatives for the rheological behavior at higher dilution rates.

3.4.5 Predicted Transport Behavior Relative to Acceptance Criteria

Reviewing the results presented in Tables 3.4 and 3.5 allows for a comparison with the CSTS Design Criteria presented in Table 3.1.

Specific Gravity

The predicted specific gravity of the slurries remains well below 1.2, much less than the 1.5 limit.

Viscosity

While the estimation method used here is not rigorous, the predicted viscosities remain well below the 30 cP design limit.

Solids Content

As mentioned earlier, if the 30% displaced solids volume is enforced as a waste acceptance criteria, this will be difficult to attain at reasonably small dilution ratios. The predicted solids volume fraction remains below 0.06 (6%) for all cases.

pH Range

As indicated in Section 2, the pH of the slurry mixtures should remain in the 11 to 14 range in all cases.

Temperature

Temperature is considered an operational variable and is not considered in this context.

Required Pressure Drop

In all cases, the pressure drop required to maintain particulate suspension is well below 500 psi (3500 kPa). This value is well below the current CSTS design limit of 1200 psi (WHC 1995).

4.0 Summary and Conclusions

This preliminary assessment has examined the potential for Tank 241-SY-102 waste properties to be adversely affected by mixing the current tank contents, by injection of additional diluent or by the heating that is expected to occur as a result of mixer pump operation during sludge mobilization. This effort has also evaluated how the transport behavior of the resulting slurries compares with the anticipated waste acceptance criteria for the CSTS.

We applied the equilibrium chemical code, GMIN, to predict potential chemical and phase equilibria. When the available chemical data were used as an input for the chemical code, modeling revealed that, while the interstitial solution can be described as being in equilibrium with the solid phase of the sludge, the supernatant liquid is clearly not in equilibrium with the solid phase. This is evidenced by the presence of solid phase species in the sludge for which relatively low concentrations (i.e., those well below the saturation value) exist in the supernatant liquid.

Since no information is currently available regarding the speciation of solids in the sludge, we selected fifteen solids as models of those that might be present there: $\text{NaNO}_3(\text{s})$, $\text{NaNO}_2(\text{s})$, thenardite, thenonatriite, $\text{NaF}(\text{s})$, sodium phosphate ($\text{Na}_3\text{PO}_4 \cdot 12\text{H}_2\text{O}(\text{s})$, $\text{Na}_3\text{PO}_4 \cdot 10\text{H}_2\text{O}(\text{s})$, and $\text{Na}_3\text{PO}_4 \cdot 8\text{H}_2\text{O}(\text{s})$), halite, gibbsite, calcite, gypsum, amorphous $\text{Cr}(\text{OH})_3$, sylvite, and amorphous SiO_2 . The relative abundance of each constituent was selected such that the measured aqueous analytes of the interstitial solution agreed (to the extent possible) with those reported by DiCenso et al. (1995), with some uncertainty on the selection of the molality of hydroxide. Reasonably good agreement was obtained between the predicted and measured molalities of the aqueous species and solids in the sludge. The model results indicate that the interstitial solution is saturated with respect to NaNO_3 , NaF , thenardite, calcite, amorphous $\text{Cr}(\text{OH})_3$, and halite. However, it is not saturated with NaNO_2 , sodium phosphate ($\text{Na}_3\text{PO}_4 \cdot 12\text{H}_2\text{O}(\text{s})$, $\text{Na}_3\text{PO}_4 \cdot 10\text{H}_2\text{O}(\text{s})$, and $\text{Na}_3\text{PO}_4 \cdot 8\text{H}_2\text{O}(\text{s})$), thenonatriite, gypsum, sylvite, and amorphous SiO_2 .

Once the sludge (both the interstitial solution and solids) and the supernate are fully mixed, the model predicts that all (or almost all) of the Na-bearing solids (i.e., $\text{NaNO}_3(\text{s})$, thenardite, $\text{NaF}(\text{s})$, and halite) are dissolved into the solution. At 50 and 75°C, the $\text{NaNO}_3(\text{s})$ is even more under-saturated than the result at 25°C, while thenardite, $\text{NaF}(\text{s})$, and halite are only somewhat farther from saturation compared with the results at 25°C.

At 25°C a small fraction of the gibbsite precipitated, but at 50 and 75°C the dissolved fraction exceeds that precipitated at the lower temperature. Thus, gibbsite precipitation may be avoided at moderate temperatures. The mixing of the sludge and supernate had little effect on the calcite and amorphous $\text{Cr}(\text{OH})_3$ at each of the temperatures considered.

We also examined the potential effects of adding pure water (as an example) to further dilute the current tank contents. This waste mixture, therefore, consists of the current sludge and supernate, plus water as a further diluent. We assumed that the additional water has the same volume as that of the supernate (932,000 L).

Similar to those of the mixture of the sludge and the supernate without additional water, the Na-bearing solids, i.e., $\text{NaNO}_3(\text{s})$, thenardite, $\text{NaF}(\text{s})$, and halite were totally dissolved at 25°C. A small amount of gibbsite was precipitated in this case, while calcite and the amorphous $\text{Cr}(\text{OH})_3$ were not significantly affected, as was the case without the additional water added.

Thus, the main conclusion of the chemical modeling based on the modeling approach is that the mixing of the sludge and the supernate (with and without additional water added) in Tank SY-102 dissolves all Na-containing solids, while the amorphous $\text{Cr}(\text{OH})_3$ and calcite phases are not affected. Finally, the gibbsite dissolved at the elevated temperatures exceeds the very small amount that might precipitate at 25°.

The chemical constituents and phase distributions predicted by the chemical modeling work were used to predict the transport behavior of the slurries which will result from sludge mobilization in Tank 102-SY. The information given in DiCenso et al. (1995) was used to predict physical and rheological properties of these slurries. These properties were compared to anticipated waste acceptance criteria for the new Hanford Cross-Site Transfer System (CSTS), based on the stated functional design criteria (WHC 1995).

An engineering correlation from the literature (that of Zandi and Govatos [1967]) was also used to estimate the critical velocity, that required to maintain slurry suspension during transport, for each slurry. Using a operating bulk transport velocity 60% greater than this critical velocity, expected pressure drops for each transfer using representative estimates of the equivalent pipe size and length.

The maximum specific gravity estimated for these slurries was well below 1.2, while the mixture viscosities were well below the 30 cP design limit. From the sedimentation information given by DiCenso et al., the displaced solids volume fraction (as discussed in Section 3.1), will likely be quite large, well above the 30% design limit for any of the cases considered. However, it is not clear that this criteria from the functional design will prove to be a waste acceptance criteria since its effects on transport behavior are unclear. The maximum volume fraction solids from the cases considered was 0.06 (6%).

The pressure drop required for transport increases with increasing temperature. However, the pressure drop for each of the cases considered was less than 500 psi (3500 kPa). This is well below the anticipated design limit of 1200 psi for the CSTS.

Issues Recommended for Additional Evaluation

A large part of the uncertainty with the chemical analyses reported in this document is related to the lack of information regarding the solid phase speciation. Should the laboratory efforts currently underway result in information which is contrary to the assumptions we have made here regarding solid phase speciation, we recommend performing some portion of these analyses again with the updated information.

This study also clearly indicated that the sludge is not in an equilibrium condition with the supernate; thus there is a need to evaluate more closely the potential for chemical reactions and associated rheology changes by incorporating spatial distributions and temporal changes of reactions and kinetics using a model which couples the physical distributions and movements with equilibrium/kinetic chemical reactions and associated rheology changes.

Since dissolution and precipitation of many of the metal hydroxide phases may occur over relatively long times (possibly days to weeks), we recommend that the effects of their kinetics be considered further.

The uncertainty associated with the transport calculations results largely from a poor understanding of the rheology of the resulting slurries, the sedimentation behavior of the solids, and, perhaps, from any uncertainty in the particle size estimates. Because of this, we recommend first reviewing the source documents that give the results of these characterizations (from which DiCenso et al. summarize). This might point to additional characterization needs.

Finally, there is almost a complete dearth of data relating slurry transport behavior in scaled transport facilities. There is a need to incorporate critical velocity and pressure drop information from tests of this type to confirm that the engineering correlations used in these analyses are appropriate. These data could be taken during experiments designed specifically for obtaining this information using waste simulants. Some information may actually be available or attainable from current or recent evaporator campaigns using actual wastes (though this may currently be limited to particular waste types). Finally, even if no other tests are performed, measurements should be obtained during actual waste transfers to verify or improve these correlations.

5.0 References

- Barney, G.S., 1976. *Vapor-Liquid-Solid Phase Equilibria of Radioactive Sodium Salt Waste at Hanford*. ARH-ST-133, Atlantic Richfield Hanford Company, Richland, Washington.
- Bunker, B. C. et al. 1995a "Colloidal Studies for Solid/Liquid Separation." *Tank Waste Treatment Science: Report for the First Quarter FY 1995*, J. P. LaFemina, ed. PNL-10762, Pacific Northwest Laboratory, Richland, Washington.
- Bunker, B. C. et al. 1995b. "Colloidal Studies for Solid/Liquid Separation," in *Tank Waste Treatment Science: Report for the Second Quarter FY 1995*, J. P. LaFemina, ed. PNL-10763, Pacific Northwest Laboratory, Richland, Washington.
- Durand, R. 1953. "Basic Relationship of the Transportation of Solids in Pipes - Experimental Research." *Proceedings, Minnesota International Hydraulics Convention*. Minneapolis, Minnesota, pp. 89-103.
- Felmy, A. R. 1990. *GMIN: A Computerized Chemical Equilibrium Model Using a Constrained Minimization of the Gibbs Free Energy*. PNL-7281, Pacific Northwest Laboratory, Richland, Washington.
- Frankel, N. A., and A. Acrivos. 1967. "On the Viscosity of a Concentrated Suspension of Solid Spheres." *Chem. Eng. Sci.*, 22:847-853.
- Glasrud, G. G., R. C. Navarrete, L. E. Scriven and C. W. Macosko. 1993. "Settling Behaviors of Iron Oxide Suspensions." *AIChE Journal*, 39(4):560-568.
- Harvie, C. E., J. P. Greenberg, and J. H. Weare. 1987. "A Chemical Equilibrium Algorithm for Highly Non-Ideal Multiphase Systems: Free Energy Minimization." *Geochemica et Cosmochimica Acta*, Vol. 51, pp. 1045-1057.
- Liu, J., L. E. Thomas, Y. L. Chen, and L. Q. Wang. 1995a. "Sludge Characterization Studies," in *Tank Waste Treatment Science: Report for the Second Quarter FY 1995*, J. P. LaFemina, ed. PNL-10763, Pacific Northwest Laboratory, Richland, Washington.
- Liu, J., L. R. Pederson, and L. Q. Wang. 1995b. *Solid-Phase Characterization in Flammable-Gas-Tank Sludges by Electron Microscopy*. PNL-10723, Pacific Northwest Laboratory, Richland, Washington.
- Mahoney, L. A., and D. S. Trent. 1995. *Correlation Models for Waste Tank Sludge and Slurries*. PNL-10695, Pacific Northwest Laboratory, Richland, Washington.
- Onishi, Y., H. C. Reid, and D. S. Trent. 1995. *Dilution Physics Modeling: Dissolution/Precipitation Chemistry*. PNL-10815, Pacific Northwest Laboratory, Richland, Washington.
- Rector, D. R. and B. C. Bunker. 1995. *Effect of Colloidal Aggregation on the Sedimentation and Rheological Properties of Tank Waste*. PNL-10761, Pacific Northwest Laboratory, Richland, Washington.
- Snoeyink, V. L., and D. Jenkins. 1980. *Water Chemistry*. John Wiley and Sons, New York.
- Westinghouse Hanford Company. 1995. *Replacement of the Cross-Site Transfer System (W-058): Functional Design Criteria*, WHC-SD-W058-FDC-001, Rev. 4, Westinghouse Hanford Company, Richland, Washington.

Zandi, I., and G. Govatos. 1967. "Heterogeneous Flow of Solids in Pipelines." *J. Hydr. Div., ASCE*, 93:HY3, Proc. Paper 5244, pp. 145-159.

Distribution

No. of
Copies

No of
Copies

OFFSITE

2 DOE Office of Scientific and Technical
Information

2 Department of Civil and Environmental
Engineering
Washington State University
Pullman, WA 99164
Attn: M. Hanaif Chaudhry
R. Y Itani

J. A. Cochran, Dean
Washington State University, Tri-Cities
Richland, WA 99352

M. Goldman
Laboratory for Energy-Related Health
Research
University of California at Davis
Davis, CA 95616

K. Kim
H. Krumb School of Mines
Columbia University
809 Seely W. Mudd
New York, NY 10027

R. B. Krone
Department of Civil and Environmental
Engineering
University of California at Davis
Davis, CA 95616-5294

S. C. T. Lien, Director, EM-54
Office of Research and Development
Office of Technology Development
Office of Environmental Management
U.S. Department of Energy
Washington, D.C. 20585

J. F. Paul
Environmental Research Laboratory
U.S. Environmental Protection Agency
Naragansett, RI 02882

D. Robey
Waterways Experimental Station
U.S. Army Corps of Engineers
Vicksburg, MS 39180

A. Schneider
Massachusetts Institute of Technology
Department of Nuclear Engineering
Room 24-1098
77 Massachusetts Avenue
Cambridge, MA 02139

G. L. Schnoor
Center for Global and Regional
Environmental Research
Civil/Environ. Engineering Dept.
University of Iowa
Iowa City, IA 52242

J. E. Till, President
Radiological Assessment Corp.
Rt. 2, Box 122
Neeses, SC 29107

U.S. Department of Energy
Trevion II Building, EM-35
Washington, D.C. 20585-0002
Attn: J. Tseng
D. Pepson

2 U.S. Environmental Protection Agency
Office of Radiation Programs
401 M Street SW
Washington, D.C. 20460
Attn: R. Dyer
K. W. Yeh

<u>No. of Copies</u>		<u>No of Copies</u>	
	Onsite		2 <u>ICF Kaiser Hanford</u>
10	<u>DOE Richland Operations Office</u>		A. N. Palit S3-05 M. A. Przybylski S2-47
	D. H. Alexander S7-51		
	S. T. Burnum S7-53	71	<u>Pacific Northwest Laboratory</u>
	R. F. Christensen S7-54		J. M. Bates K7-15
	J. J. Davis S6-62		S. Q. Bennett K7-90
	R. E. Gerton S7-54		J. W. Brothers K5-22
	C. A. Groendyke S7-54		R. M. Ecker K6-91
	G. A. Meyer S2-48		A. R. Felmy K9-77
	B. L. Nicoll S7-53		J. A. Fort K7-15
	G. W. Rosenwald S7-54		M. D. Freshley P8-34
	W. R. Wrzesinski S7-53		P. A. Gauglitz P7-41
26	<u>Westinghouse Hanford Company</u>		G. R. Golcar P7-20
	H. Babad S7-30		W. W. Laity P7-27
	G. S. Barney T5-12		L. M. Liljegren K7-15
	W. B. Barton H5-21		L. K. Holton K9-73
	K. G. Carothers R1-51		J. D. Hudson (10) K7-15
	J. L. Gilbert B4-08		W. L. Kuhn K2-21
	J. P. Harris S6-12		J. P. Lafemina K2-25
	D. L. Herting T6-09		M. A. Lilga P8-38
	J. D. Hopkins R2-11		T. E. Michener K7-15
	G. D. Johnson S7-15		Y. Onishi (30) K9-33
	J. W. Lentsch S7-15		F. E. Panisko P8-34
	J. M. Light B4-08		L. R. Pederson K2-44
	E. J. Lipke S7-14		M. R. Powell P7-14
	D. A. Reynolds R2-11		B. A. Reynolds P7-19
	C. A. Rieck (5) R3-27		R. K. Quinn K9-69
	G. J. Rust T4-01		H. C. Reid K7-15
	M. J. Sutey T4-07		J. R. Rustad K9-77
	J. E. VanBeek (5) R3-27		W. D. Samuels K2-44
	R. J. Van Vleet H4-62		C. W. Stewart K7-15
			D. S. Trent K7-15
			Information Release (5)